Design Framework & Concepts for 6D Cooling After Rectilinear Yield (6D CARY)

Cary Y. Yoshikawa

Outline

- Purpose
- Preliminaries: Figure of Merit for σ_E
- Motivation/Inspiration of Design
- Evolution of Design
- Asymptotic Performance Reach Using an Initial Attempt at Coping with Rectilinear Transverse Emittance
- Updated Methods to Cope with Rectilinear Transverse Emittance
- Summary

Purpose

The intent is to present a design framework and concepts for additional 6D cooling beyond that achieved by the Rectilinear channel and have this archived for potential further development if deemed worth pursuing and funding becomes available.

Preliminaries: Figure of Merit for σ_E

Evaluation of the energy spread will be based on an energy spread evolution formula in Dave Neuffer's 1999 CERN yellow paper (CERN 99-15, 16 Decemeber 1999):

$$\frac{d\sigma_E^2}{ds} = -2\frac{g_L(dE/ds)}{\beta^2 E}\sigma_E^2 + 4\pi(r_e m_e c^2)^2 n_e \gamma^2\left(1-\frac{\beta^2}{2}\right) . \quad (4.9)$$

- The longitudinal partition number g_L increases as $\eta\rho'/\rho_0$, where η is the dispersion and ρ'/ρ_0 is the relative change in density with respect to transverse position. All configurations will use wedges with uniform density, so $g_L = \eta$.
- r_e is the classical electron radius $2.82\text{x}10^{-15}$ m.
- n_e is the electron density in the material (LiH).
  - $n_e = N_A\rho Z/A = (6.02\text{x}10^{23}\ /g) \text{ x } (8.2\text{x}10^{8}\ g/m^3) \text{ x } (0.50321) = 2.48\text{x}10^{29}\ /m^3$

➢ Setting the above derivative to zero provides the energy spread equilibrium.

$$\sigma_E|_{Eq} = \beta\gamma(r_e m_e c^2)\sqrt{\frac{2\pi n_e\left(1-\frac{\beta^2}{2}\right)E}{\eta(\frac{dE}{ds})}}$$

Preliminaries: Figure of Merit for σ_E

Exact use of $\sigma_{E|Eq}$ wasn't clear. Is it the standard deviation or full width?

$$\sigma_E|_{Eq} = \beta\gamma(r_e m_e c^2)\sqrt{\frac{2\pi n_e\left(1-\frac{\beta^2}{2}\right)E}{\eta(\frac{dE}{ds})}}$$

Looked at last stage of Rectilinear output for guidance/benchmark and apparently the full width seems to fit, so will use it this way.

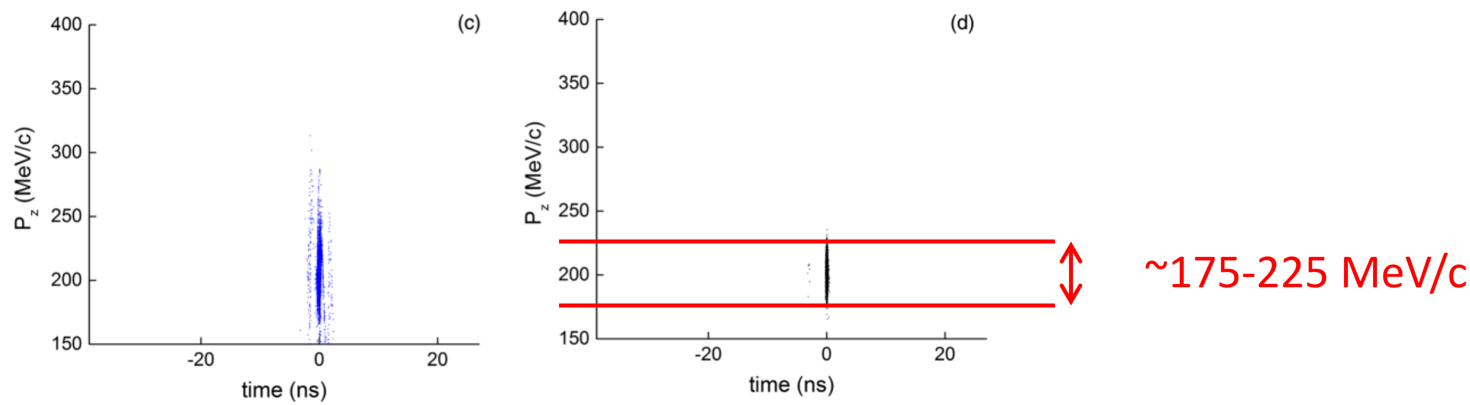

FIG. 8. Snapshots of a sample of the longitudinal phase space at various positions along our proposed 6D rectilinear cooling channel: (a) at the entrance of the cooling channel before recombination; (b) at the entrance of the bunch merger; (c) at the exit of the bunch merger [26]; (d) at the end of the 6D cooling channel.

ΔP = ~175-225 MeV/c ➡ ΔE = ~204.4-248.6 MeV = 44.2 MeV

$\sigma_E|_{Eq}(\eta = 6\,mm) = 39.9\,MeV$

Assuming the last stage of the Rectilinear channel strives for the equilibrium energy spread, we'll assume the calculated $\sigma_{E|Eq}$ is reasonable for the **full width** in our evaluations. Even if not exactly correct, it at least provides a consistent measure.

Motivation/Inspiration of Design

As noted above, better longitudinal cooling can be achieved with larger dispersion and the initial design attempts to exploit this.

$$\sigma_E|_{Eq} = \beta\gamma(r_e m_e c^2)\sqrt{\frac{2\pi n_e\left(1-\frac{\beta^2}{2}\right)E}{\boldsymbol{\eta}(\frac{dE}{ds})}}$$

An old study (MOPP071 EPAC08) for capturing pions/muons off a target for a potential Mu2e upgrade utilized a Dipole/Wedge scheme that involved very large dispersion (1.15 m) and monochromized the beam in a single pass.

Evolution of the design discovers another dimension in longitudinal emittance reduction…or at least containment.

Motivation of Design (MOPP071 EPAC08)

$$\eta = \frac{\Delta x}{\frac{\Delta p}{p_0}} = 1.15\ \text{m}$$

Rectilinear: 6mm

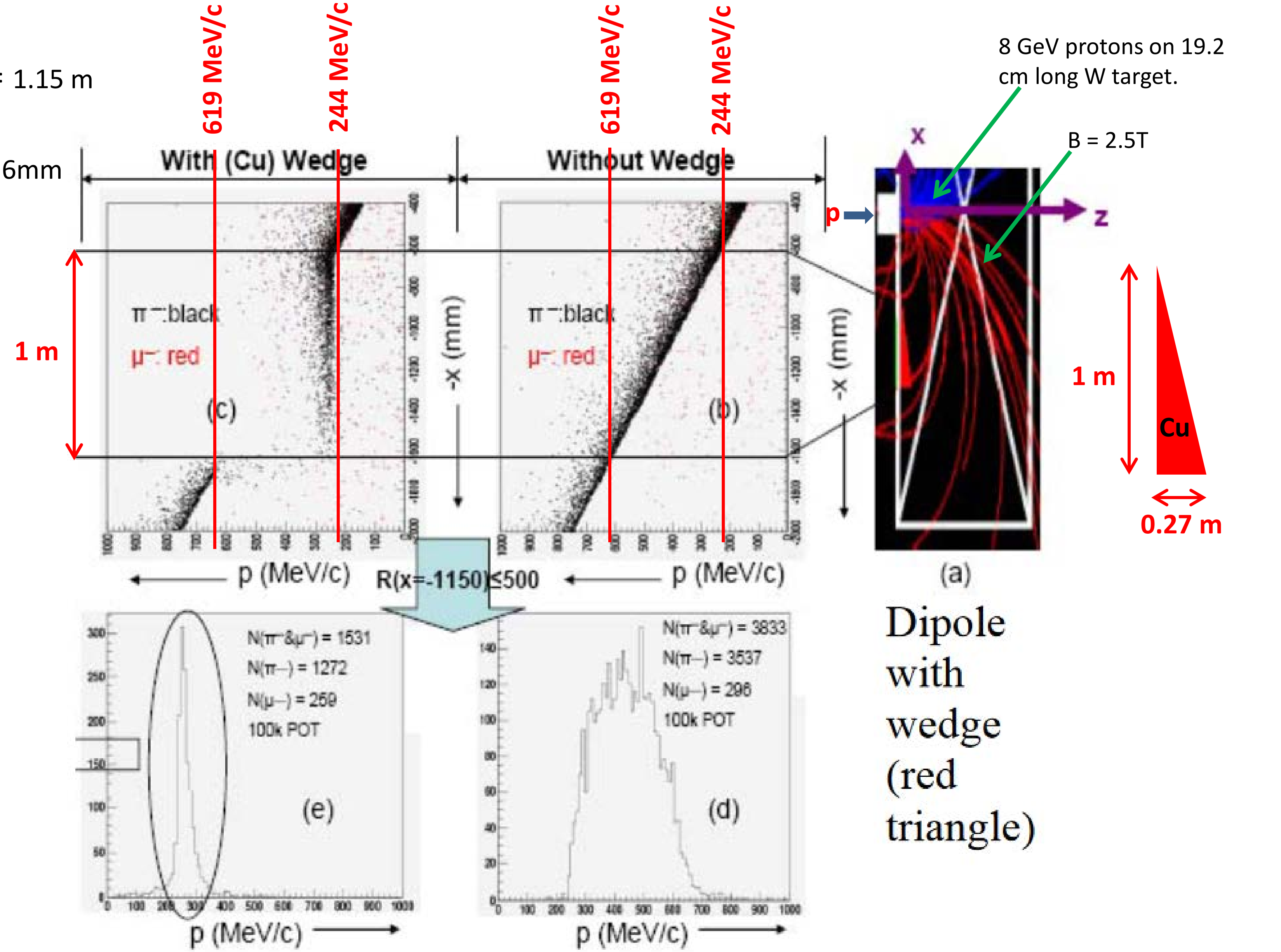

Dipole with wedge (red triangle)

Motivation of Design (MOPP071 EPAC08)

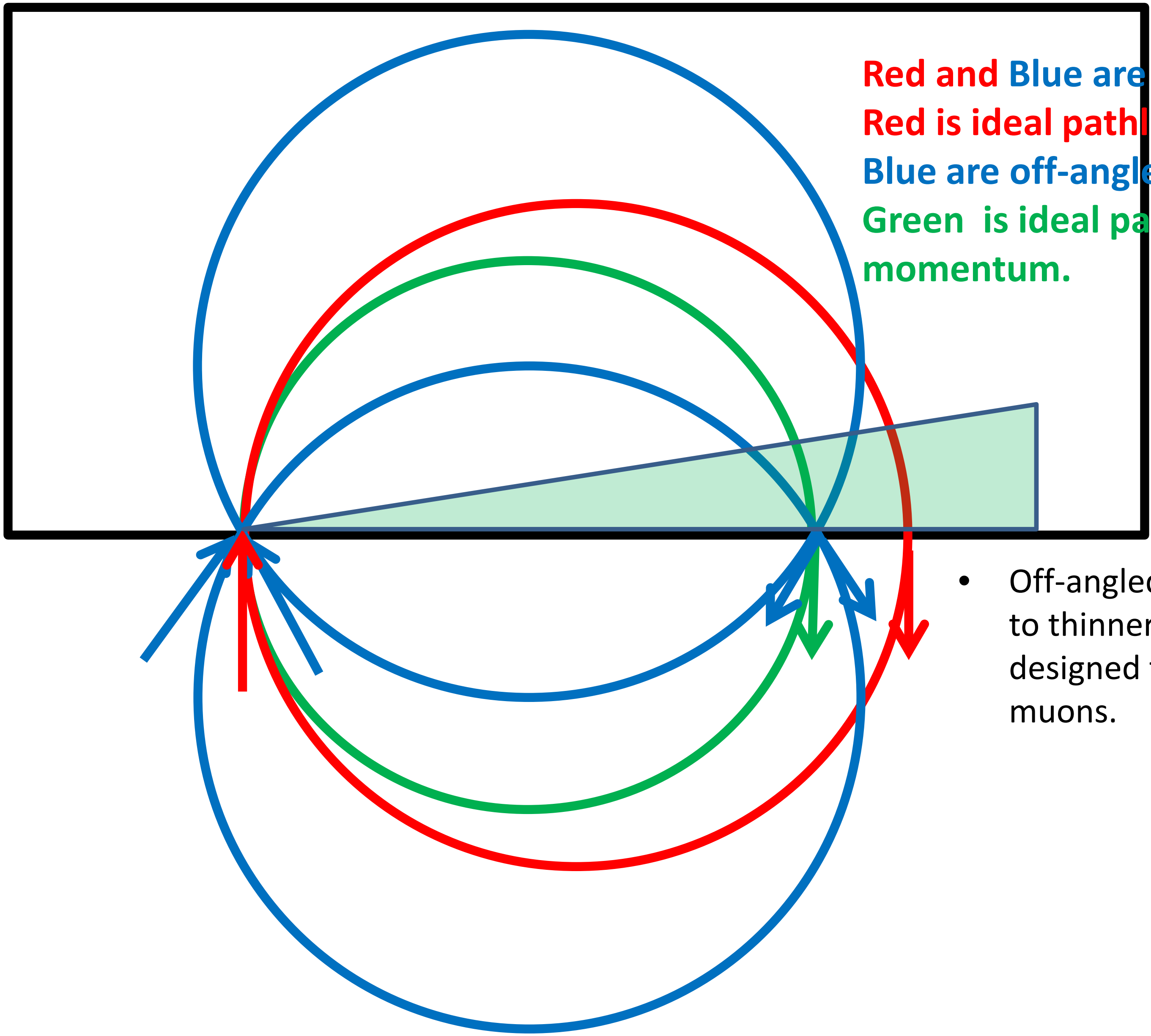

Red and Blue are same momenta.
Red is ideal path.
Blue are off-angled.
Green is ideal path of lower momentum.

- Off-angled muons are directed to thinner parts of the wedge designed for lower momenta muons.

Design I: Based on EPAC08

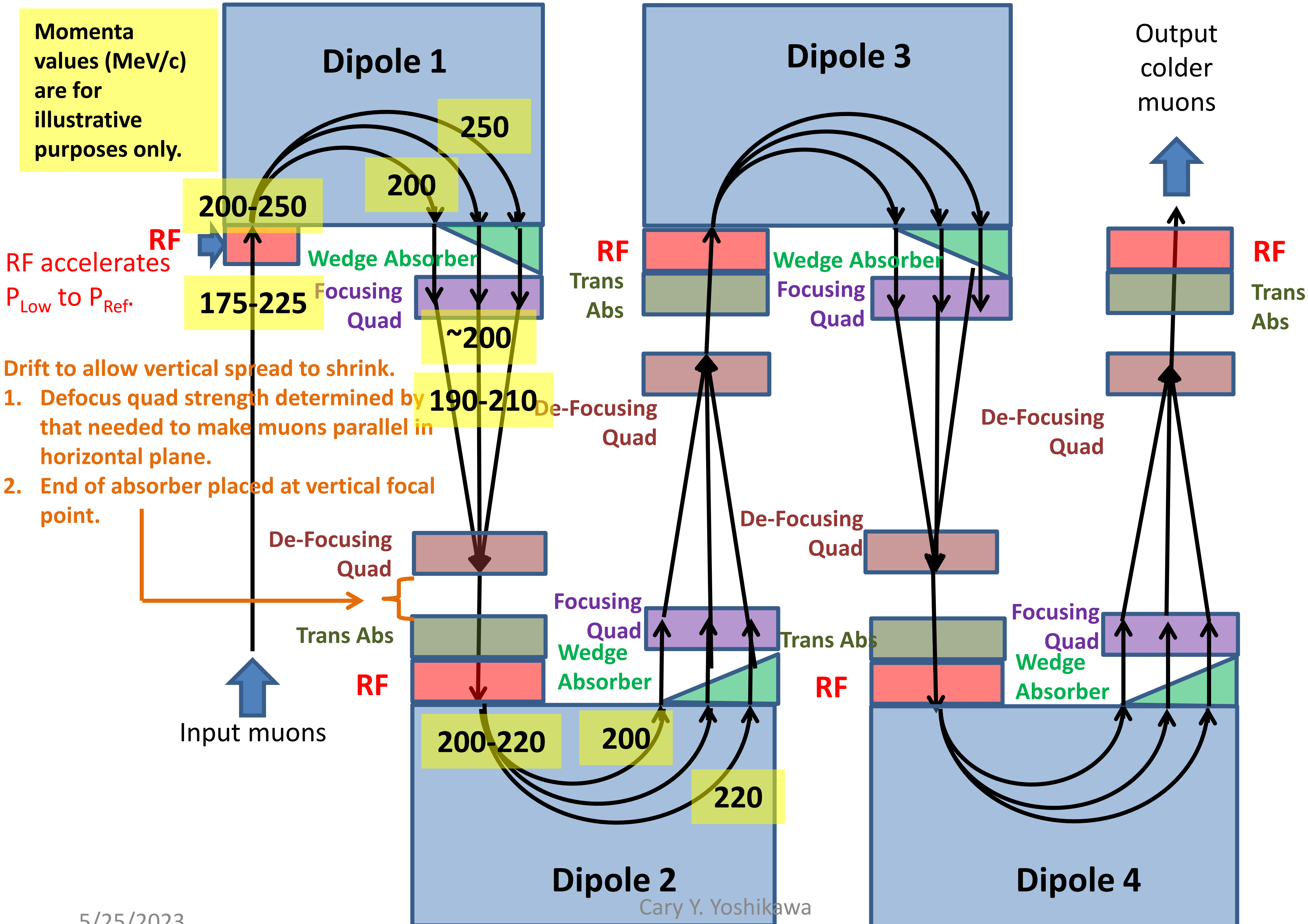

Design II: 90^o Bend to Create Space for Components

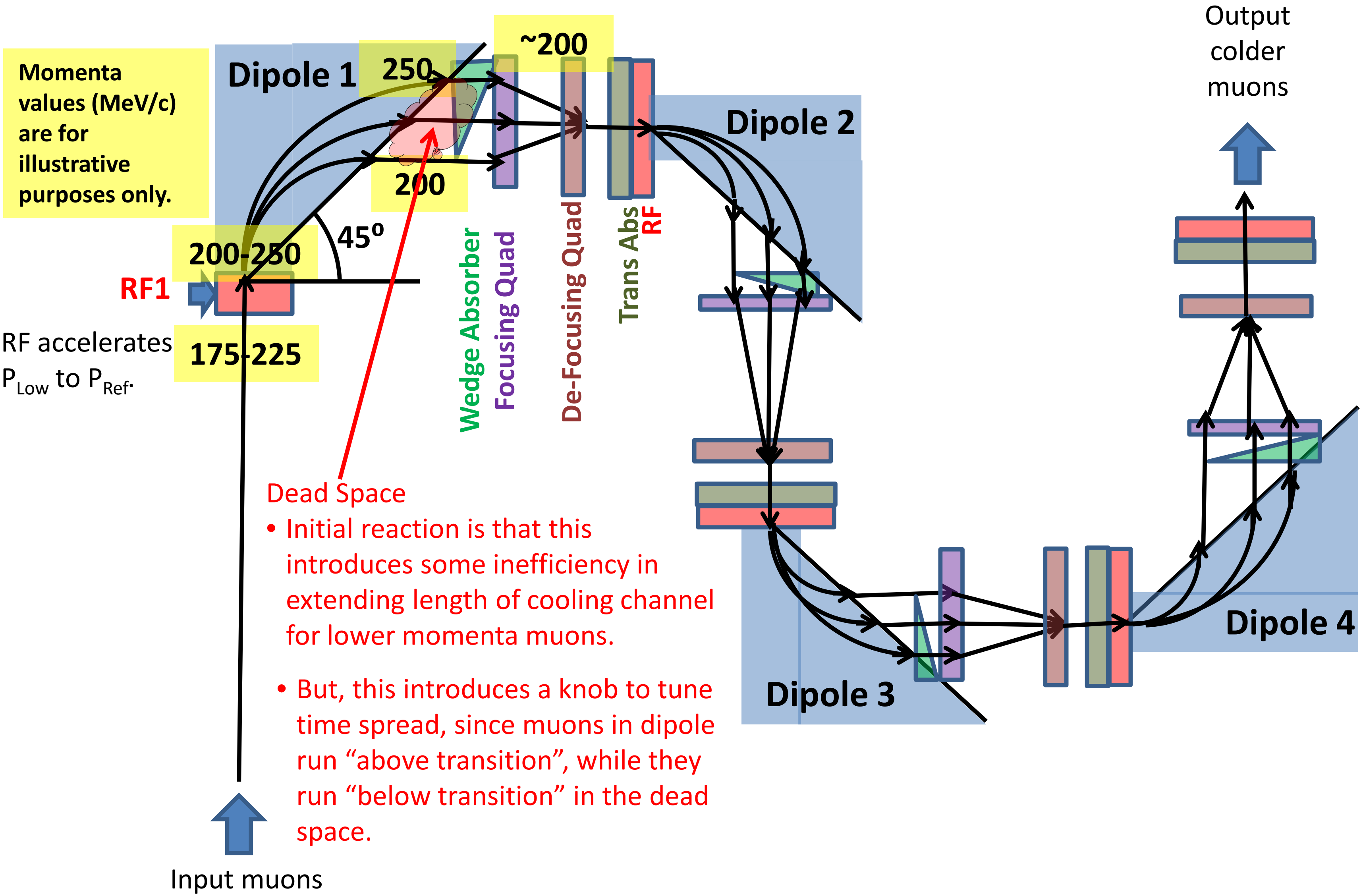

Dead Space

- Initial reaction is that this introduces some inefficiency in extending length of cooling channel for lower momenta muons.
- But, this introduces a knob to tune time spread, since muons in dipole run "above transition", while they run "below transition" in the dead space.

Design III: Isochronicity

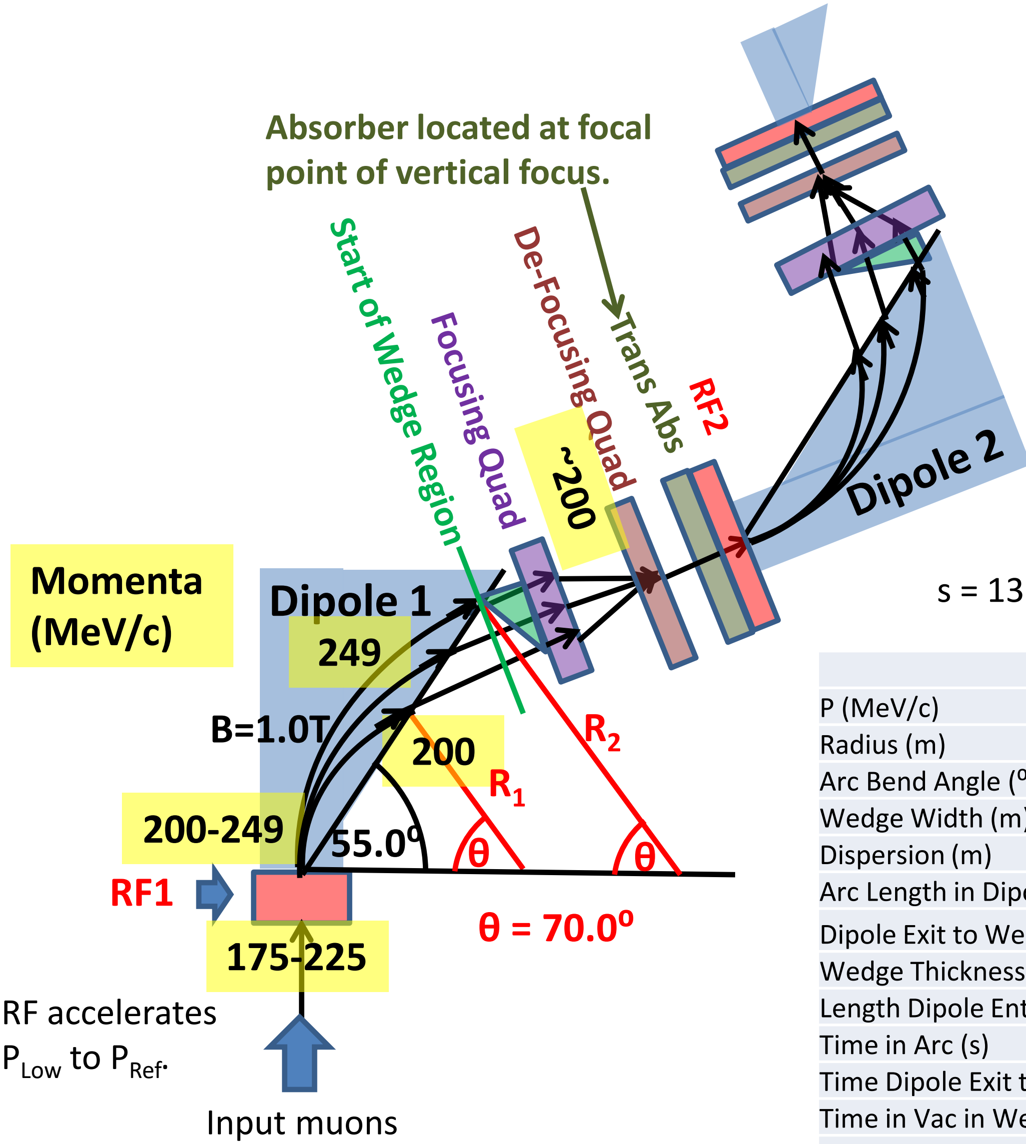

Isochronous Condition:

$$\left[\frac{R_2}{v_2} - \frac{R_1}{v_1}\right]\theta - \frac{(R_2-R_1)}{v_1}\sin\theta + t_{2,LiH} - \frac{D}{v_1} = 0$$

D = 27.12 cm for 249 -> 200 MeV/c in LiH.

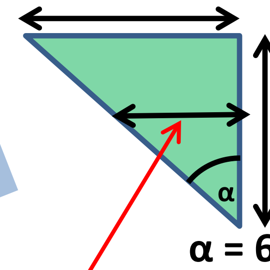

$w = \Delta R\sqrt{2(1-\cos\theta) - \sin^2\theta} = 10.7$ cm

End of Rectilinear channel:
- Apex angle is 120°
- Dispersion is 0.006 m.

s = 13.28 cm for 224 -> 200 MeV/c in LiH.

	Low	Mid	High
P (MeV/c)	200.00	224.42	248.84
Radius (m)	0.667	0.748	0.829
Arc Bend Angle (°)		69.979	
Wedge Width (m)		0.107	
Dispersion (m)		0.492	
Arc Length in Dipole (m)	0.814	0.914	1.013
Dipole Exit to Wedge Region Start (m)	0.153	0.076	0.000
Wedge Thickness (m)		0.271	
Length Dipole Entry to Wedge Exit (m)	1.238	1.261	1.284
Time in Arc (s)	3.07E-09	3.37E-09	3.67E-09
Time Dipole Exit to Wedge Region Start (s)	5.77E-10	2.82E-10	0
Time in Vac in Wedge Region (s)	1.02E-09	5.10E-10	0
Time in LiH in Wedge Region (s)	0	4.95E-10	1.00E-09
Time Dipole Entry to Wedge Exit (s)	4.67E-09	4.66E-09	4.67E-09

Time over 27.12 cm – 13.28 cm = 13.84 cm

Design III: Isochronicity

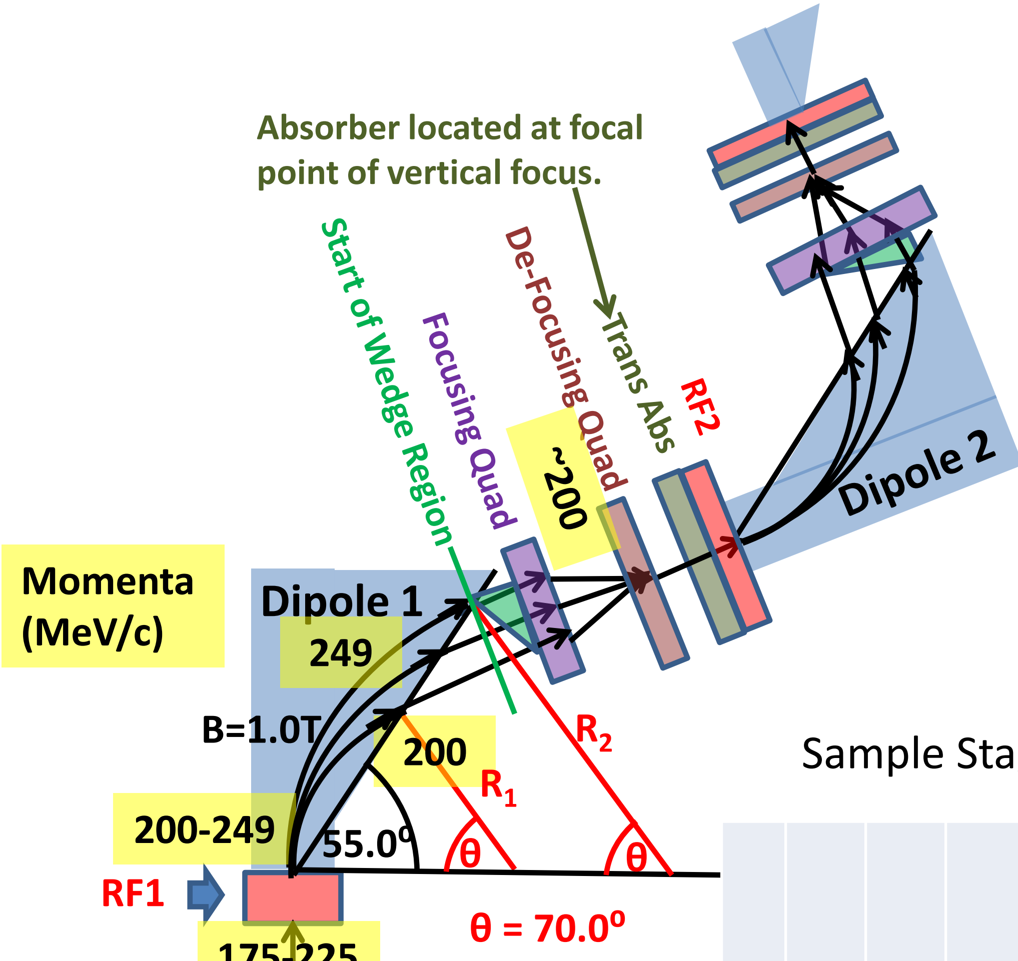

RF accelerates P_{Low} to P_{Ref}.

Input muons

Note that $\sigma_{E|Eq}$ is smaller for longer configurations using lower B fields. But, large input transverse emittance will restrict initial configurations to be smaller.

Isochronous Condition:

$$\left[\frac{R_2}{v_2} - \frac{R_1}{v_1}\right]\theta - \frac{(R_2 - R_1)}{v_1}\sin\theta + t_{2,LiH} - \frac{D}{v_1} = 0$$

D = 27.12 cm for 249 -> 200 MeV/c in LiH.

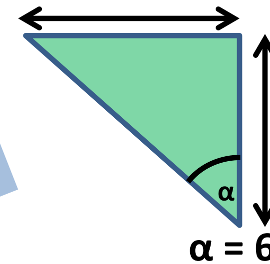

$w = \Delta R\sqrt{2(1-\cos\theta) - \sin^2\theta} = 10.7$ cm

End of Rectilinear channel:

- Apex angle is 120°
- Dispersion is 0.006 m.
- $\sigma_{E|Eq}$ = 39.92 MeV

Sample Stage 1 Configuration Options

B(T)	R_1 (m)	R_2 (m)	W_{Wedge} (m)	Dispersion (m)	$\sigma_{E\|Eq}$ (MeV)	Opening Angle from Dipole Entry to Wedge Exit (°)	θ (°)	α (°)	Path Len To Wedge Exit (m) 200 MeV/c	Path Len To Wedge Exit (m) 249 MeV/c
0.50	1.33	1.66	0.201	0.9255	3.21	5.27	67.58	53.40	2.145	2.228
0.75	0.89	1.11	0.139	0.6368	3.88	5.05	68.81	62.93	1.541	1.599
1.00	0.67	0.83	0.107	0.4920	4.41	4.86	69.98	68.46	1.238	1.284
2.00	0.33	0.41	0.059	0.2725	5.92	4.27	74.24	77.67	0.781	0.809

Design III: Isochronicity

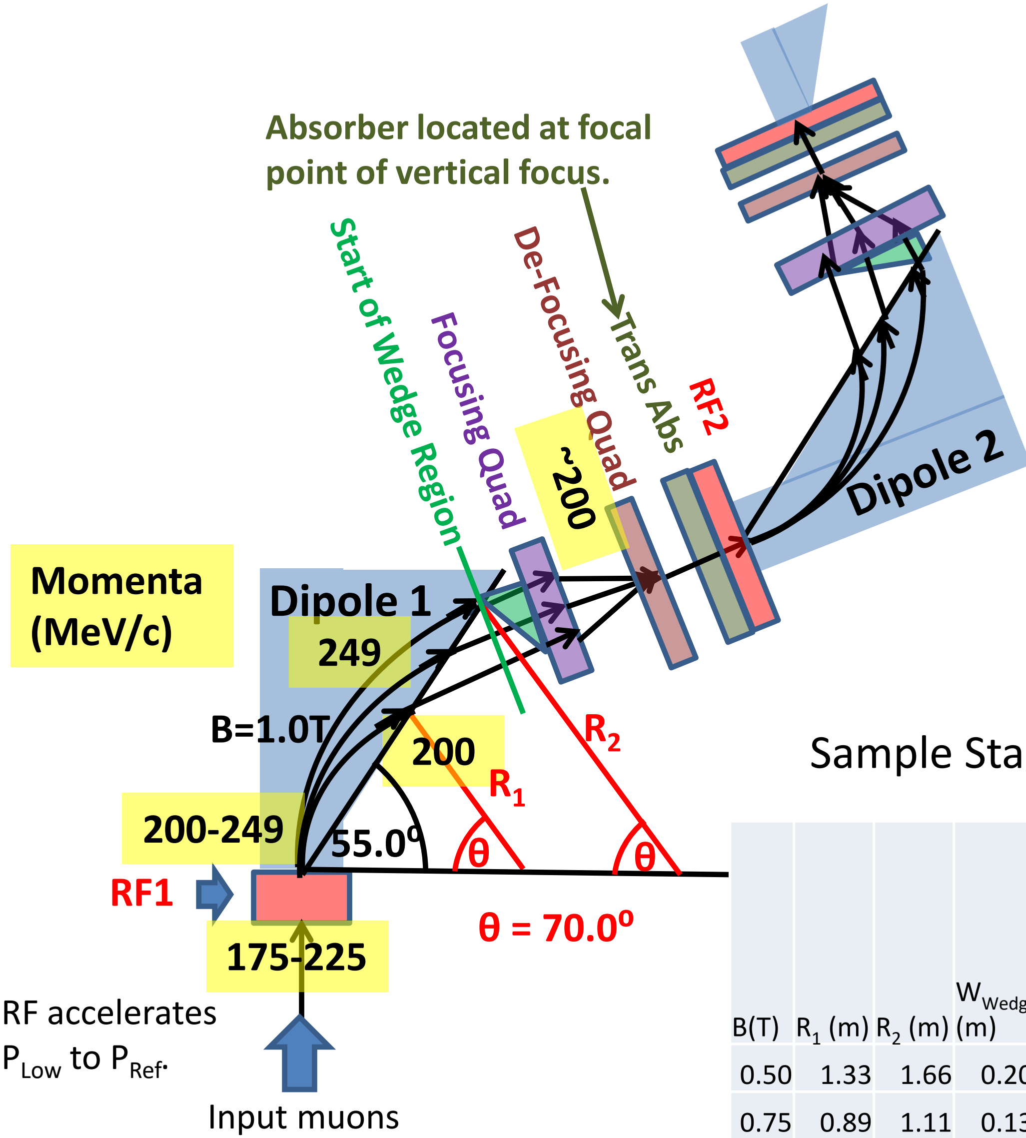

Isochronous Condition:

$$\left[\frac{R_2}{v_2} - \frac{R_1}{v_1}\right]\theta - \frac{(R_2 - R_1)}{v_1}\sin\theta + t_{2,LiH} - \frac{D}{v_1} = 0$$

D = 27.12 cm for 249 -> 200 MeV/c in LiH.

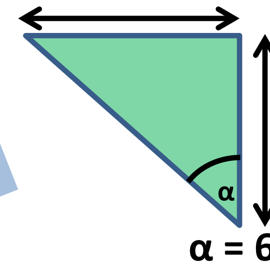

$w = \Delta R\sqrt{2(1-\cos\theta) - \sin^2\theta} = 10.7$ cm

End of Rectilinear channel:

- Apex angle is 120°
- Dispersion is 0.006 m.
- $\sigma_{E|Eq}$ = 39.92 MeV

Sample Stage 1 Configuration Options

B(T)	R_1 (m)	R_2 (m)	W_{Wedge} (m)	Dispersion (m)	$\sigma_{E\|Eq}$ (MeV)	Opening Angle from Dipole Entry to Wedge Exit (°)	θ (°)	α (°)	Path Len To Wedge Exit (m) 200 MeV/c	Path Len To Wedge Exit (m) 249 MeV/c
0.50	1.33	1.66	0.201	0.9255	3.21	5.27	67.58	53.40	2.145	2.228
0.75	0.89	1.11	0.139	0.6368	3.88	5.05	68.81	62.93	1.541	1.599
1.00	0.67	0.83	0.107	0.4920	4.41	4.86	69.98	68.46	1.238	1.284
2.00	0.33	0.41	0.059	0.2725	5.92	4.27	74.24	77.67	0.781	0.809

Simple Geometric Argument for Wedge Configuration for Minimal Energy Spread

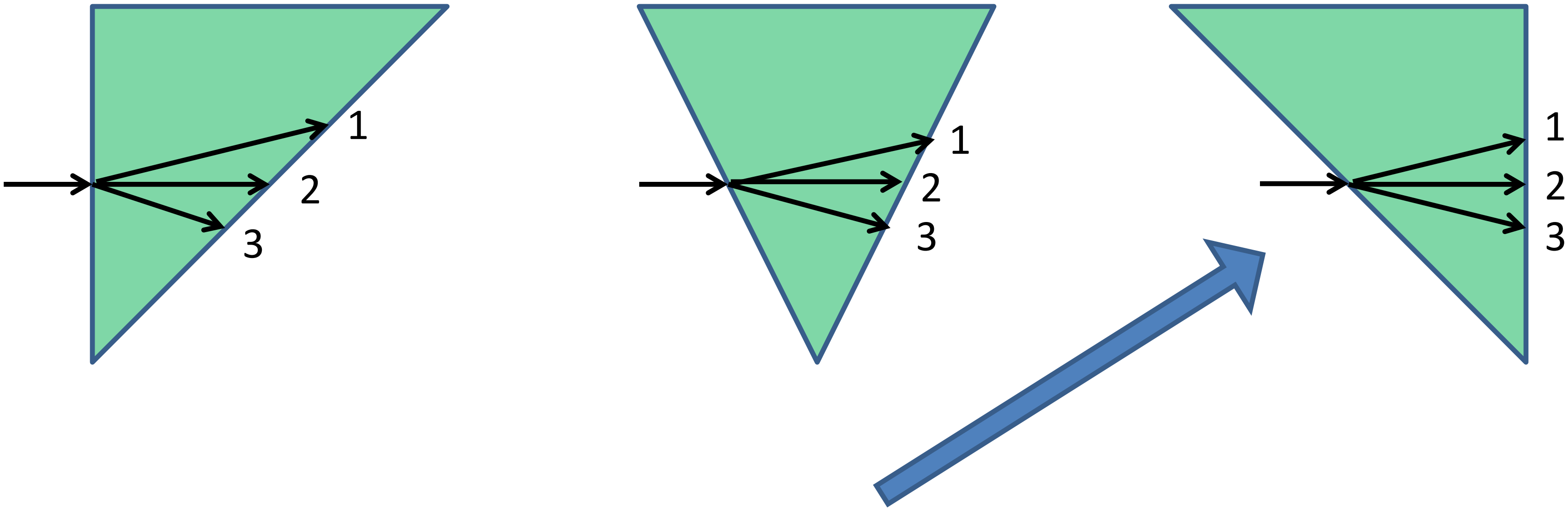

The configuration to the right should have minimal energy spread compared to the other two wedges due to expected smaller path differences between the 3 particle trajectories.

Timing Considerations for Wedge Configuration

- Note that among the 3 configurations below, the left that introduces absorber earliest has timing for P_{Mid} closest to P_{High} & P_{Low}.
- If reduction of time spread becomes a higher priority than energy spread, a configuration as one to the left might be used.
- Further time spread reduction might be realized by introducing the slowing absorber material earlier between the dipole exit and wedge region entry.
- Might even be desirable to have P_{Mid} be later than P_{High} & P_{Low}, since path length for P_{Mid} will be shorter than those for P_{High} & P_{Low} from focusing quad to defocusing quad.

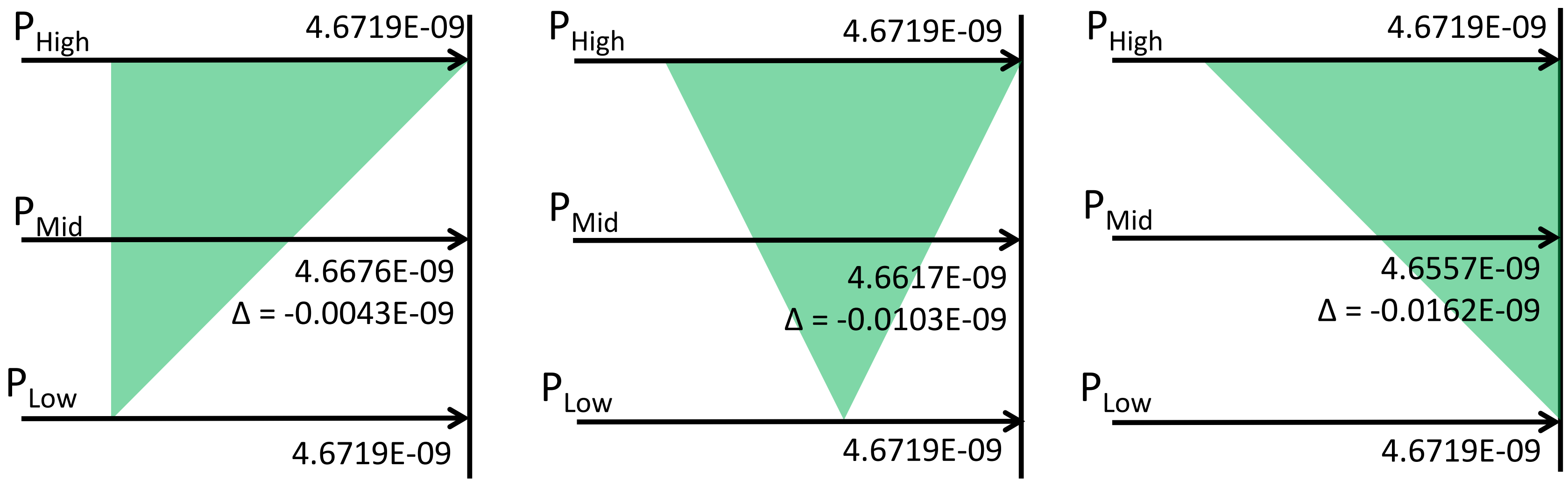

- For now, energy spread reduction will be the priority and the configuration to the right above will be used.

Design III: Isochronicity

➢ **Last Stage Ends at RF**

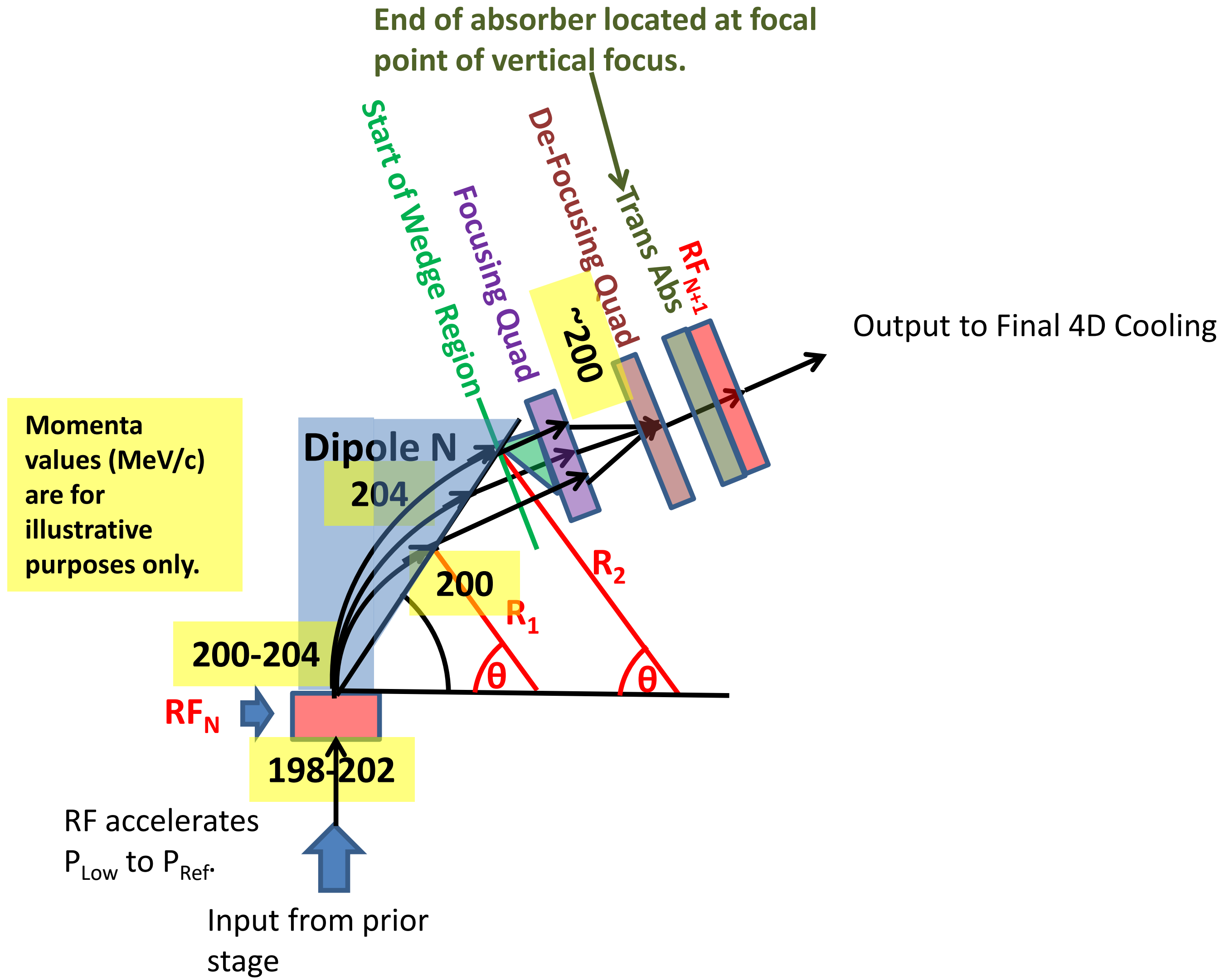

Impact of Upstream Transverse Emittance

Angular span from dipole entry to end of wedge:

θx = 2 x tan-1((W/2)/L) = 4.86 degrees

	Rectilinear [A]	Rectilinear [B]
$\varepsilon_{T,N}$ (mm)	0.28	0.3
$\varepsilon_{L,N}$ (mm)	1.57	1.58
$\Delta\theta_x = 2\tan^{-1}[(\Delta P_x/2)/P_z]$ (deg)	33.40	22.62
Pz (MeV/c)	200	200
ΔPx (MeV/c)	120	80

[A] Stratakis & Palmer PRLSTAB 18, 031003 (2015)

[B] Zhu Ruihu, Muon Cooling Working Group Meeting, 2023.03.23

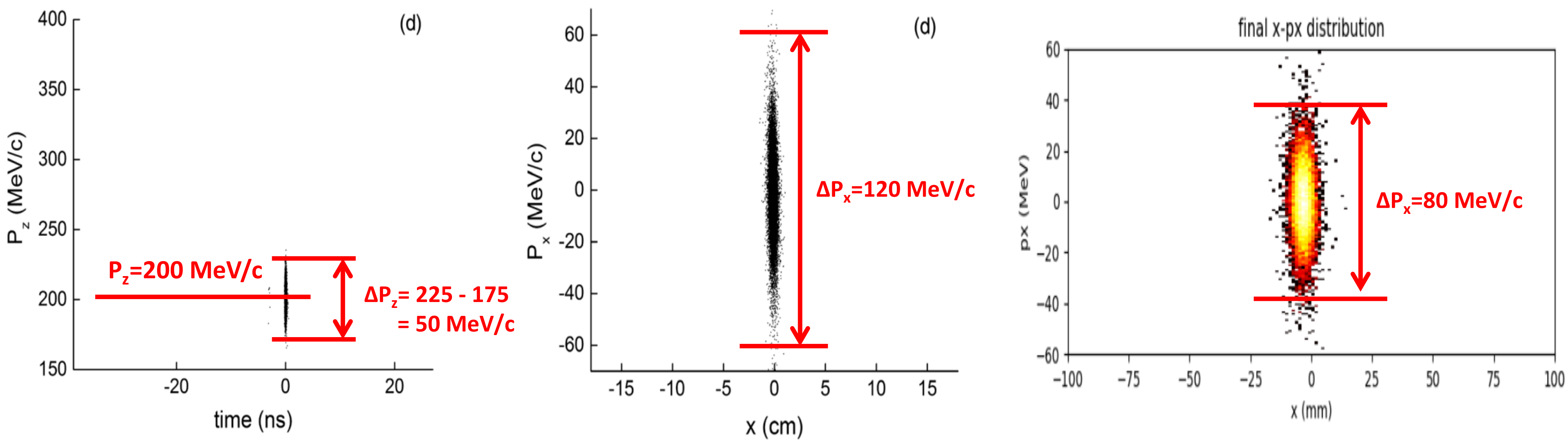

Impact of Upstream Transverse Emittance

Angular span from dipole entry to end of wedge:

θx = 2 x tan-1((W/2)/L) = 4.86 degrees

	Rectilinear [A]	Rectilinear [B]
$\varepsilon_{T,N}$ (mm)	0.28	0.3
$\varepsilon_{L,N}$ (mm)	1.57	1.58
$\Delta\theta_x = 2\tan^{-1}[(\Delta P_x/2)/P_z]$ (deg)	33.40	22.62
Pz (MeV/c)	200	200
ΔPx (MeV/c)	120	80

[A] Stratakis & Palmer PRLSTAB 18, 031003 (2015)

[B] Zhu Ruihu, Muon Cooling Working Group Meeting, 2023.03.23

At end of Rectilinear, beam spread at absorber is 10.7 times the size of the sensitive area for cooling between P = 175 to 225 MeV/c.

Dispersion η (m)	0.0060
$\Delta x_{Abs} = \eta \frac{\Delta p}{p_0}$(m)	0.0015
Δx,beam from Fig 9d (m)	0.0160
$\Delta x_{,beam}/\Delta x_{Abs}$	10.6667

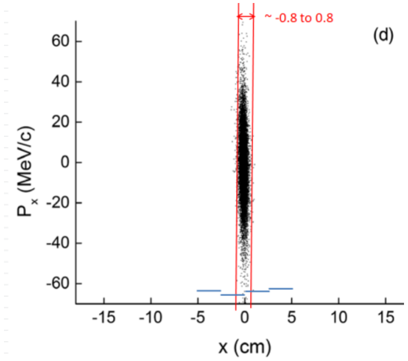

So, cooling a beam that spans beyond the designed sensitive region appears to work!

The following slides will present:

1. Schemes (not necessarily advocated in the final result) that attempt to address the effect of the large transverse spread of the beam from the Rectilinear channel by introducing absorber material above and below the designed wedge region.
2. Calculations of such schemes using configurations that are not able to directly address the large transverse spread out of the Rectilinear channel, but does provide asymptotic results, assuming that the transverse spread can be managed in the earlier stages.
3. Updated Methods to Cope with Rectilinear Transverse Emittance

- ➢ Item 3 provides methods to accommodate the Rectilinear channel output, while items 1 & 2 provide the asymptotic reach of this post-Rectilinear 6D cooling system.

Modified Enlarged Wedge Geometry

- Strategy to handle the large transverse spread out of the Rectilinear channel output is to transversely extend the reach of the wedge absorber material, while maintaining the designed energy loss for muons with zero angular spread.
- Design is driven by desire to address the expected non-trivial amount of large angle muons with $P > P_{Low,Plus}$ that travel below wedge. If no absorber exists below the wedge, these particles go unimpeded and would likely compromise the cooling performance significantly.
- Note that large angle muons with $P > P_{Low,Plus}$ that travel below wedge will traverse more material due to the large angles, helping it migrate to desired P_{Low}, while unfortunately large angle muons with $P < P_{High,Plus}$ that travel above the wedge will loose more energy than desired, migrating away from desired P_{Low}.
- Question is how much material to add after the green wedge to set value of $P_{Low,Plus}$. Too much material lengthens the absorber which forces it to widen as well in order to maintain the angular acceptance and a wider absorber leads to a wider focusing quad. So, desire least amount of material that can help mitigate large number of muons with $P>P_{Low,Plus}$ and large angles.

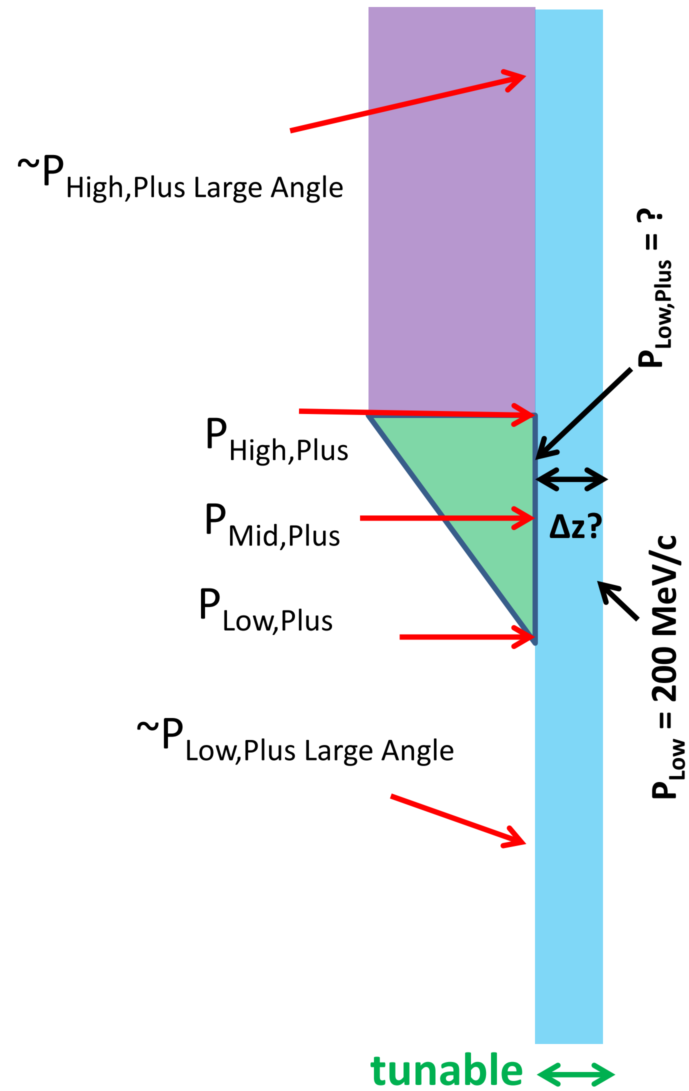

Modified Enlarged Wedge Geometry

For now, we choose 5.35 cm of LiH which will cool 210 MeV/c muons down to 200 MeV/c. This can be optimized in later studies.

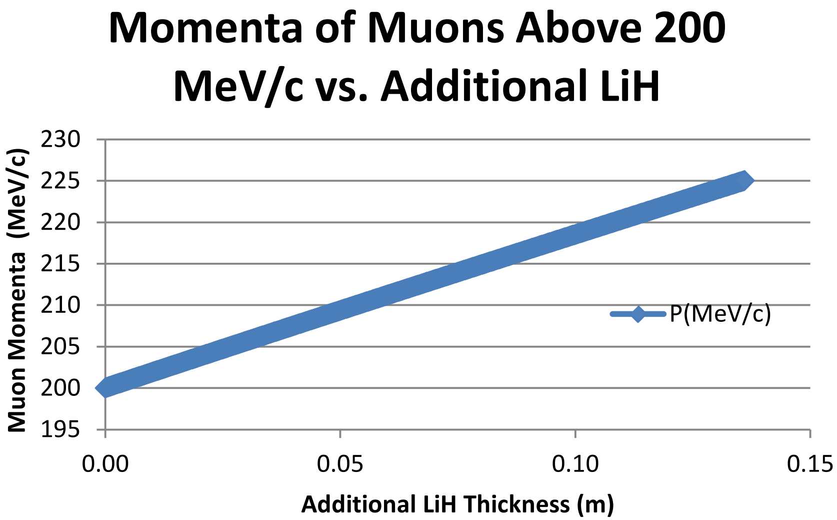

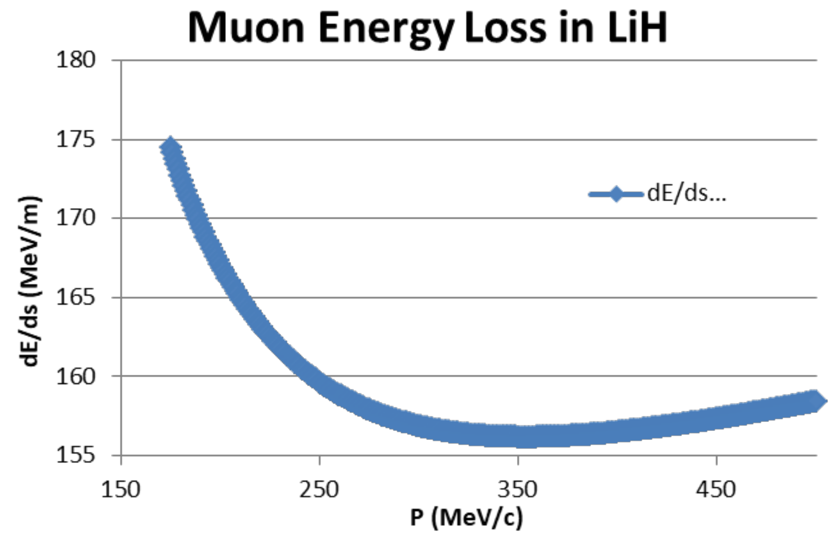

Sample Stage 1 Configuration Options ($P_{Low,Plus}$ = 210 MeV/c, $P_{High, Plus}$ = 258 MeV/c)

B (T)	R1 (m)	R2 (m)	W_{Wedge} (m)	Dispersion (m)	$\sigma_{E\|Eq}$ (MeV)	Opening Angle from Dipole Entry to Wedge Exit (°)	θ (°)	α (°)	Path Len to Wedge Exit (m) 210 MeV/c	Path Len to Wedge Exit (m) 258 MeV/c	Path Len to Wedge Exit (m) Avg	$\Delta W_{HighOrLow}$ (m) [A]	$W_{Mod\ Wedge}$ (m) [B]
0.500	1.400	1.723	0.18629	0.9003	3.26	4.76	64.94	63.91	2.207	2.280	2.243	0.44866	1.08361
0.750	0.933	1.149	0.12822	0.6196	3.93	4.51	66.12	71.37	1.601	1.653	1.627	0.32536	0.77894
1.000	0.700	0.862	0.09908	0.4788	4.47	4.31	67.25	75.40	1.297	1.338	1.318	0.26355	0.62619
1.518	0.461	0.568	0.06904	0.3337	5.35	3.95	69.44	79.71	0.985	1.015	1.000	0.20000	0.46904
2.000	0.350	0.431	0.05493	0.2654	6.00	3.70	71.33	81.78	0.839	0.863	0.851	0.17024	0.39540

Note that the vertical spread is 2 x 0.2m = 0.4m, while the horizontal is 0.469m, which would define the quad aperture.

A: $\Delta W_{HighOrLow} = L_{avg}\ [(\Delta Px/2)/Pz]$

B: $W_{Mod\ Wedge} = W_{Wedge} + 2\ \Delta W_{HighOrLow}$

ΔPx = 80 MeV/c

Pz = 200 MeV/c

Design IV: Isochronicity with Modified Wedge

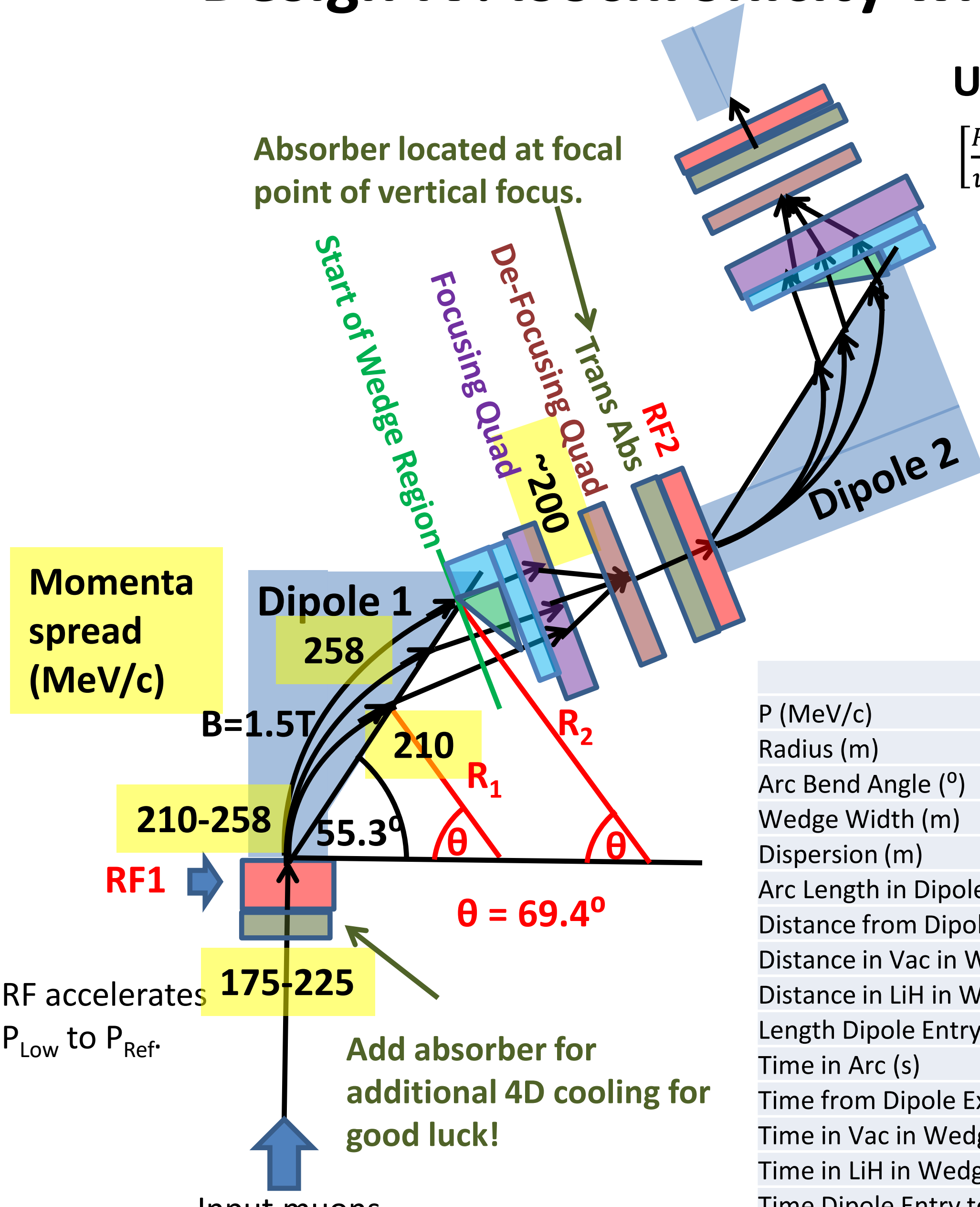

Updated Isochronous Condition:

$$\left[\frac{R_2}{v_2}-\frac{R_1}{v_1}\right]\theta - \frac{(R_2-R_1)}{v_1}\sin\theta + t_{2,LiH} - \frac{(D_2-D_1)}{v_1} - t_{1,LiH} = 0$$

D_2 = 32.69 cm for 258 -> 200 MeV/c in LiH.

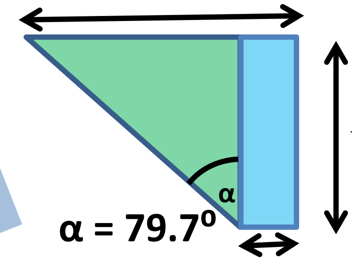

$w = \Delta R\sqrt{2(1-\cos\theta) - \sin^2\theta}$ =6.9 cm

D_1 = 5.35 cm for 210 -> 200 MeV/c in LiH.

End of Rectilinear channel:

- Apex angle is 120°
- Dispersion is 0.006 m

	Low	Mid	High
P (MeV/c)	210.00	234.24	258.47
Radius (m)	0.461	0.514	0.568
Arc Bend Angle (°)		69.436	
Wedge Width (m)		0.0690	
Dispersion (m)		0.3337	
Arc Length in Dipole (m)	0.5588	0.6233	0.6878
Distance from Dipole Exit to Wedge Region Entry (m)	0.0996	0.0498	0.0000
Distance in Vac in Wedge Region (m)	0.2734	0.1390	0.0000
Distance in LiH in Wedge Region (m)	0.0535	0.1879	0.3269
Length Dipole Entry to Wedge Exit (m)	0.9853	1.0000	1.0147
Time in Arc (s)	2.09E-09	2.28E-09	2.48E-09
Time from Dipole Exit to Wedge Region Entry (s)	3.72E-10	1.82E-10	0.00E+00
Time in Vac in Wedge Region (s)	1.02E-09	5.09E-10	0.00E+00
Time in LiH in Wedge Region (s)	2.01E-10	6.97E-10	1.20E-09
Time Dipole Entry to Wedge Exit (s)	3.68E-09	3.67E-09	3.68E-09

First 10 Sequential Stages

Below are parameters and momenta/energy values for the first 10 stages designed sequentially where the output of a stage drives the design of the subsequent stage. Note that it'll take approximately a dozen stages to reduce the beam spread $\sigma_{E,Out}$ to midway between the initial value of 44.15 MeV from the Rectilinear channel and the initial equilibrium of 5.35 MeV in stage 1.

Stage	PLow,In (MeV/c)	PHigh,In (MeV/c)	B (T)	R1 (m) PLow	R2 (m) PHigh	Dispersion η (m)	Arc Bend θ (deg)	Wedge Width (m)	Wedge D1 (m)	Wedge D2 (m)	Path Len To Wedge Exit (m) PLow	Path Len To Wedge Exit (m) PMid	Path Len To Wedge Exit (m) PHigh	σE,Out (MeV)	σE|Eq (MeV)	ELow, Out (MeV)	EHigh, Out (MeV)	ΔE for RF [A] (MeV)	PLow, Out (MeV/c)	PHigh, Out (MeV/c)	σP,Out (MeV/c)
Rectilinear						0.006								44.15	39.92	204.42	248.57		175.00	225.00	50.00
1	210.00	258.47	1.518	0.461	0.568	0.334	69.436	0.069	0.0535	0.3269	0.9853	1.0000	1.0147	41.92	5.35	205.23	247.16	30.66	175.94	223.43	47.49
2	210.00	256.06	1.467	0.477	0.582	0.340	69.068	0.067	0.0535	0.3129	0.9858	1.0000	1.0142	39.84	5.30	206.27	246.11	29.85	177.16	222.28	45.12
3	210.00	253.81	1.422	0.492	0.595	0.347	68.741	0.065	0.0535	0.2998	0.9862	1.0000	1.0138	37.89	5.25	207.25	245.14	28.81	178.29	221.20	42.91
4	210.00	251.70	1.381	0.507	0.607	0.352	68.453	0.064	0.0535	0.2876	0.9867	1.0000	1.0133	36.07	5.21	208.16	244.23	27.83	179.35	220.19	40.84
5	210.00	249.72	1.345	0.520	0.619	0.358	68.196	0.062	0.0535	0.2762	0.9871	1.0000	1.0129	34.36	5.17	209.02	243.37	26.92	180.34	219.24	38.90
6	210.00	247.86	1.312	0.534	0.630	0.363	67.964	0.060	0.0535	0.2655	0.9875	1.0000	1.0125	32.76	5.13	209.82	242.57	26.07	181.27	218.35	37.08
7	210.00	246.12	1.282	0.546	0.640	0.368	67.757	0.058	0.0535	0.2555	0.9879	1.0000	1.0121	31.25	5.09	210.57	241.82	25.27	182.14	217.52	35.38
8	210.00	244.48	1.255	0.558	0.649	0.373	67.569	0.057	0.0535	0.2461	0.9883	1.0000	1.0117	29.85	5.06	211.27	241.12	24.52	182.95	216.73	33.78
9	210.00	242.95	1.231	0.569	0.658	0.378	67.400	0.055	0.0535	0.2373	0.9887	1.0000	1.0113	28.52	5.03	211.93	240.46	23.81	183.72	216.00	32.28
10	210.00	241.50	1.209	0.579	0.666	0.382	67.250	0.053	0.0535	0.2291	0.9891	1.0000	1.0109	27.28	5.00	212.55	239.83	23.15	184.43	215.31	30.87

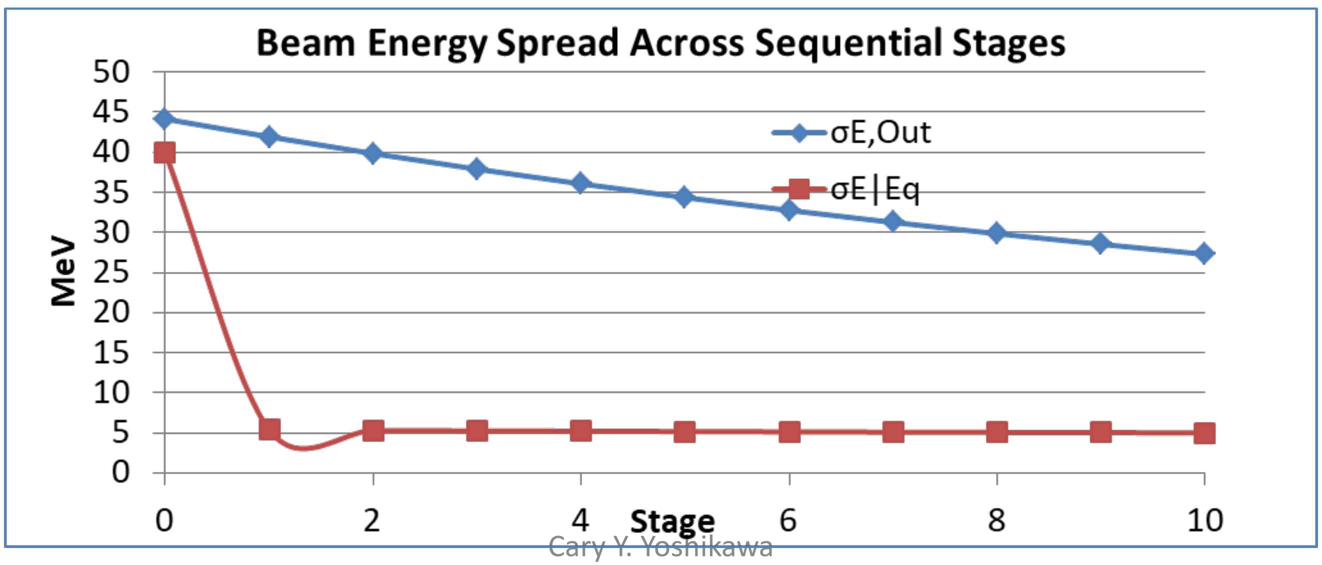

[A] ΔE for energy loss in 4D absorber is not included.

Grouped Stages

To expedite investigation of viability of parameters and performance of subsequent stages, we assumed any particular stage could be reused until $\sigma_{E,Out}$ was reduced to midway between $\sigma_{E,Init}$ and $\sigma_{E|Eq}$, which would define $\sigma_{E,Init}$ for the subsequent stage. We'll refer to the reused stages as a stage group.

Stage Group	$P_{Low,In}$ (MeV/c)	$P_{High,In}$ (MeV/c)	B (T)	R1 (m) P_{Low}	R2 (m) P_{High}	Dispersion η (m)	Arc Bend θ (deg)	Wedge Width (m)	Wedge D1 (m)	Wedge D2 (m)	Path Len To Wedge Exit (m) P_{Low}	Path Len To Wedge Exit (m) P_{Mid}	Path Len To Wedge Exit (m) P_{High}	$\sigma_{E,Out}$ (MeV)	$\sigma_{E\|Eq}$ (MeV)	ELow, Out (MeV)	EHigh, Out (MeV)	ΔE for RF [A] (MeV)	PLow, Out (MeV/c)	PHigh, Out (MeV/c)	σP, Out (MeV/c)
Rectilinear						0.006								44.150	39.923	204.42	248.57		175.00	225.00	50.00
1	210.00	258.47	1.518	0.461	0.568	0.334	69.436	0.0690	0.0535	0.3269	0.9853	1.0000	1.0147	24.752	5.354	213.82	238.57	30.66	185.89	213.90	28.01
2	210.00	237.38	1.148	0.610	0.689	0.394	66.844	0.0482	0.0535	0.2056	0.9902	1.0000	1.0098	14.839	4.926	218.77	233.61	21.26	191.57	208.35	16.79
3	210.00	226.49	1.003	0.698	0.753	0.429	65.850	0.0324	0.0535	0.1411	0.9935	1.0000	1.0065	9.781	4.723	221.30	231.08	16.31	194.45	205.51	11.06
4	210.00	220.89	0.946	0.740	0.778	0.446	65.637	0.0225	0.0535	0.1132	0.9955	1.0000	1.0045	7.206	4.631	222.59	229.80	13.78	195.92	204.07	8.15
5	210.00	218.04	0.917	0.763	0.793	0.455	65.487	0.0171	0.0535	0.0974	0.9966	1.0000	1.0034	5.895	4.583	223.25	229.14	12.49	196.66	203.33	6.67
6	210.00	216.58	0.902	0.776	0.800	0.460	65.418	0.0142	0.0535	0.0894	0.9972	1.0000	1.0028	5.227	4.559	223.58	228.81	11.84	197.04	202.95	5.91
7	210.00	215.84	0.895	0.782	0.804	0.463	65.383	0.0127	0.0535	0.0853	0.9975	1.0000	1.0025	4.887	4.547	223.75	228.64	11.50	197.23	202.76	5.53
8	210.00	215.46	0.891	0.785	0.806	0.464	65.366	0.0119	0.0535	0.0832	0.9976	1.0000	1.0024	4.713	4.540	223.84	228.55	11.33	197.33	202.66	5.33
9	210.00	215.26	0.890	0.787	0.807	0.465	65.359	0.0115	0.0535	0.0822	0.9977	1.0000	1.0023	4.625	4.537	223.88	228.51	11.25	197.38	202.61	5.23
10	210.00	215.17	0.889	0.788	0.807	0.465	65.353	0.0113	0.0535	0.0816	0.9978	1.0000	1.0022	4.580	4.535	223.90	228.48	11.20	197.41	202.59	5.18

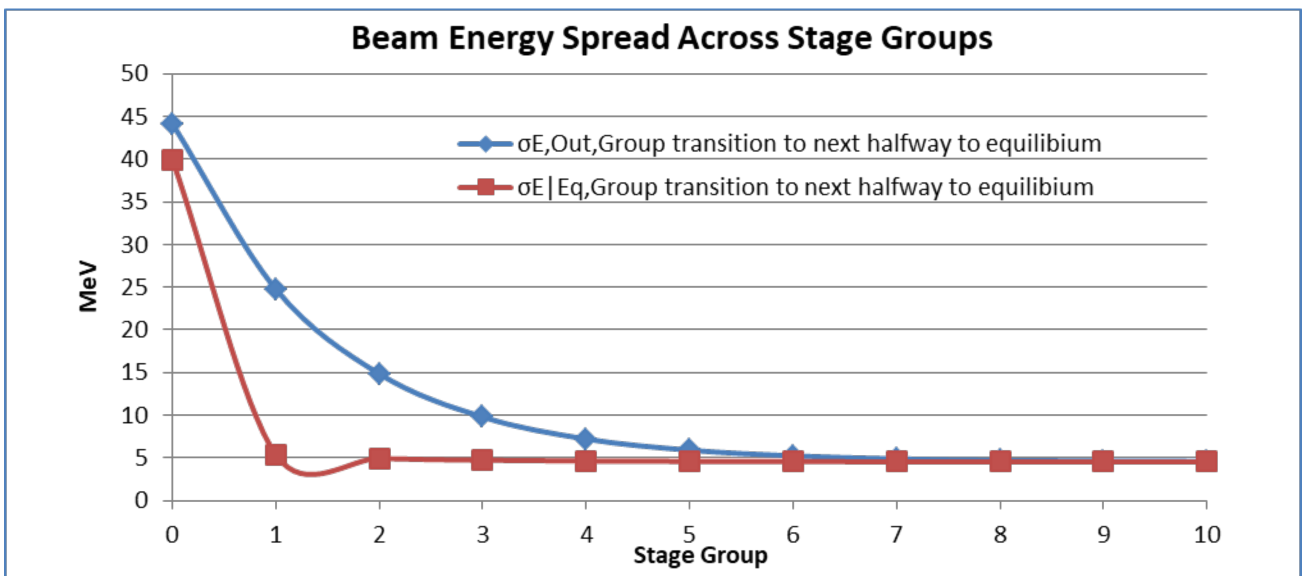

[A] ΔE for energy loss in 4D absorber is not included.

Potential Improvement with Smaller Transverse Emittance Downstream

As transverse emittance is reduced, the smaller angular beam spread will allow reach to larger dispersion via a longer distance from dipole entry to the wedge exit. To estimate the sensitivity of improvement, L_{Mid} is increased from 1m to 2m for stage groups ≥ 4.

Stage Group	PLow,In (MeV/c)	PHigh,In (MeV/c)	B (T)	R1 (m) PLow	R2 (m) PHigh	Dispersion η (m)	Arc Bend θ (deg)	Wedge Width (m)	Wedge D1 (m)	Wedge D2 (m)	Path Len To Wedge Exit (m) PLow	Path Len To Wedge Exit (m) PMid	Path Len To Wedge Exit (m) PHigh	σE,Out (MeV)	$\sigma_E\vert_{Eq}$ (MeV)	ELow, Out (MeV)	EHigh,Out (MeV)	ΔE for RF [A] (MeV)	PLow, Out (MeV/c)	PHigh, Out (MeV/c)	σP,Out (MeV/c)
Rectilinear						0.006								44.150	39.923	204.42	248.57		175.00	225.00	50.00
1	210.00	258.47	1.518	0.461	0.568	0.334	69.436	0.0690	0.0535	0.3269	0.9853	1.0000	1.0147	24.752	5.354	213.82	238.57	30.66	185.89	213.90	28.01
2	210.00	237.38	1.148	0.610	0.689	0.394	66.844	0.0482	0.0535	0.2056	0.9902	1.0000	1.0098	14.839	4.926	218.77	233.61	21.26	191.57	208.35	16.79
3	210.00	226.49	1.003	0.698	0.753	0.429	65.850	0.0324	0.0535	0.1411	0.9935	1.0000	1.0065	9.781	4.723	221.30	231.08	16.31	194.45	205.51	11.06
4	210.00	220.89	0.441	1.589	1.671	0.941	65.015	0.0476	0.0535	0.1132	1.9906	2.0000	2.0094	6.484	3.187	222.95	229.44	13.78	196.33	203.66	7.33
5	210.00	217.23	0.430	1.629	1.685	0.958	65.050	0.0324	0.0535	0.0930	1.9936	2.0000	2.0064	4.822	3.159	223.78	228.60	12.13	197.27	202.72	5.45
6	210.00	215.38	0.424	1.650	1.692	0.967	65.072	0.0245	0.0535	0.0828	1.9952	2.0000	2.0048	3.983	3.145	224.20	228.19	11.30	197.74	202.25	4.51
7	210.00	214.45	0.422	1.661	1.696	0.971	65.084	0.0204	0.0535	0.0777	1.9960	2.0000	2.0040	3.561	3.138	224.41	227.97	10.88	197.98	202.01	4.03
8	210.00	213.98	0.423	1.655	1.686	0.971	65.263	0.0182	0.0535	0.0832	1.9964	2.0000	2.0036	3.349	3.138	224.52	227.87	10.67	198.10	201.89	3.79
9	210.00	213.74	0.420	1.669	1.698	0.975	65.095	0.0172	0.0535	0.0739	1.9966	2.0000	2.0034	3.241	3.133	224.57	227.81	10.56	198.17	201.83	3.67
10	210.00	213.62	0.419	1.670	1.699	0.975	65.096	0.0167	0.0535	0.0732	1.9967	2.0000	2.0033	3.186	3.132	224.60	227.79	10.51	198.20	201.80	3.60

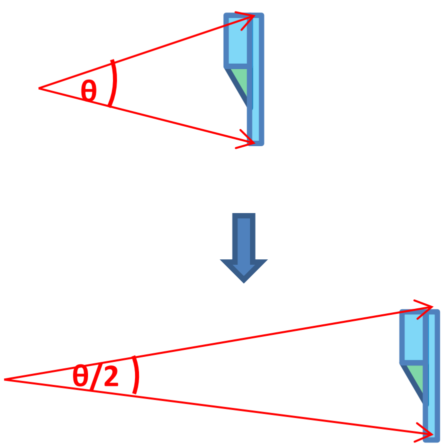

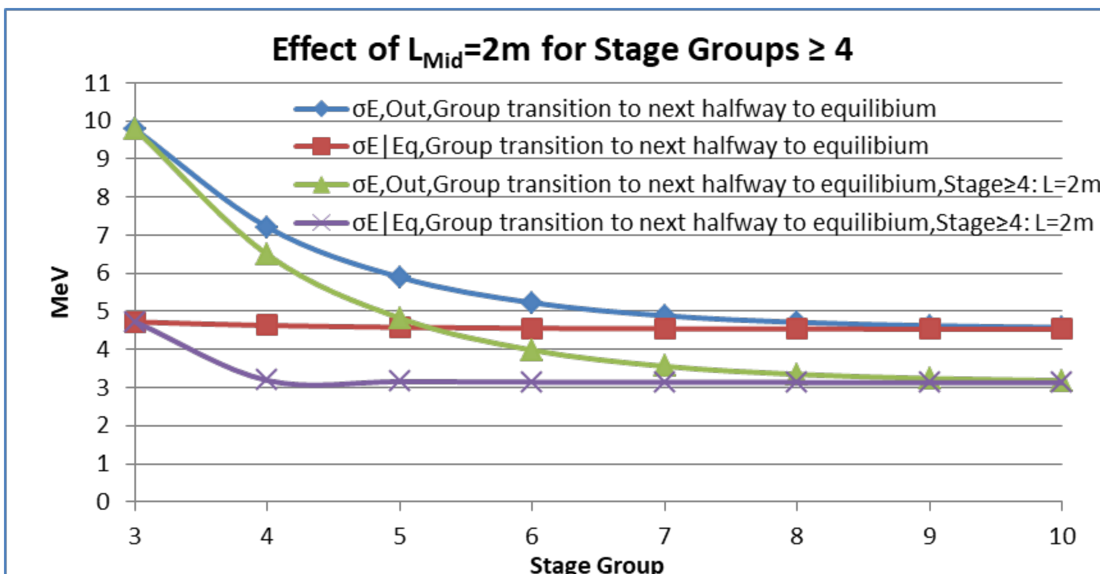

[A] ΔE for energy loss in 4D absorber is not included.

Potential Improvement with Thinner Absorber Downstream

As longitudinal emittance is reduced, the smaller momenta spread suggests lowering the raised P_{Low} starting point which means a thinner absorber (smaller D1) and a slight increase in length that determines isochronicity at start of D1. This increases slightly the wedge width & dispersion. Below, D1 ≈ D2 / 2 for stage groups ≥ 5. Improvement is incremental.

Stage Group	PLow,In (MeV/c)	PHigh,In (MeV/c)	B (T)	R1 (m) PLow	R2 (m) PHigh	Dispersion η (m)	Arc Bend θ (deg)	Wedge Width (m)	Wedge D1 (m)	Wedge D2 (m)	Path Len To Wedge Exit (m) PLow	Path Len To Wedge Exit (m) PMid	Path Len To Wedge Exit (m) PHigh	σE,Out (MeV)	σE|Eq (MeV)	ELow, Out (MeV)	EHigh, Out (MeV)	ΔE for RF [A] (MeV)	PLow, Out (MeV/c)	PHigh, Out (MeV/c)	σP,Out (MeV/c)
Rectilinear						0.006								44.150	39.923	204.42	248.57		175.00	225.00	50.00
1	210.00	258.47	1.518	0.461	0.568	0.334	69.436	0.0690	0.0535	0.3269	0.9853	1.0000	1.0147	24.752	5.354	213.82	238.57	30.66	185.89	213.90	28.01
2	210.00	237.38	1.148	0.610	0.689	0.394	66.844	0.0482	0.0535	0.2056	0.9902	1.0000	1.0098	14.839	4.926	218.77	233.61	21.26	191.57	208.35	16.79
3	210.00	226.49	1.003	0.698	0.753	0.429	65.850	0.0324	0.0535	0.1411	0.9935	1.0000	1.0065	9.781	4.723	221.30	231.08	16.31	194.45	205.51	11.06
4	210.00	220.89	0.441	1.589	1.671	0.941	65.637	0.0476	0.0535	0.1132	1.9906	2.0000	2.0094	6.484	3.187	222.95	229.44	13.78	196.33	203.66	7.33
5	207.33	214.59	0.426	1.623	1.680	0.973	65.754	0.0335	0.0391	0.0785	1.9933	2.0000	2.0067	4.809	3.134	223.79	228.60	9.75	197.28	202.72	5.44
6	205.44	210.83	0.418	1.640	1.683	0.993	66.288	0.0257	0.0290	0.0580	1.9948	2.0000	2.0052	3.956	3.103	224.22	228.17	7.23	197.76	202.23	4.47
7	204.47	208.92	0.413	1.648	1.684	1.004	66.567	0.0216	0.0238	0.0477	1.9956	2.0000	2.0044	3.521	3.087	224.43	227.95	5.94	198.01	201.99	3.98
8	203.98	207.94	0.411	1.653	1.685	1.009	66.709	0.0194	0.0212	0.0424	1.9961	2.0000	2.0039	3.300	3.079	224.54	227.84	5.29	198.13	201.86	3.73
9	203.73	207.44	0.410	1.655	1.685	1.012	66.782	0.0183	0.0198	0.0397	1.9963	2.0000	2.0037	3.187	3.075	224.60	227.79	4.96	198.20	201.80	3.60
10	203.60	207.19	0.410	1.656	1.685	1.013	66.821	0.0177	0.0192	0.0384	1.9964	2.0000	2.0036	3.130	3.073	224.63	227.76	4.79	198.23	201.77	3.54

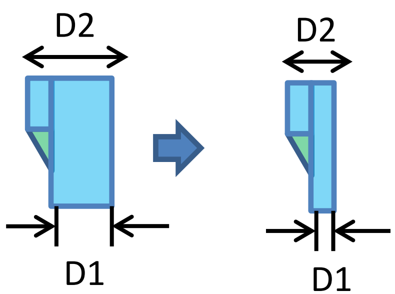

- Dispersion is continuous.
- Highest density of muons will be at the wedge.
- Muons above wedge encounter twice as much absorber than below it.
- Overall $\sigma_{E|Eq}$ reduction from Rectilinear is from 39.9 MeV to ~3.1 MeV.

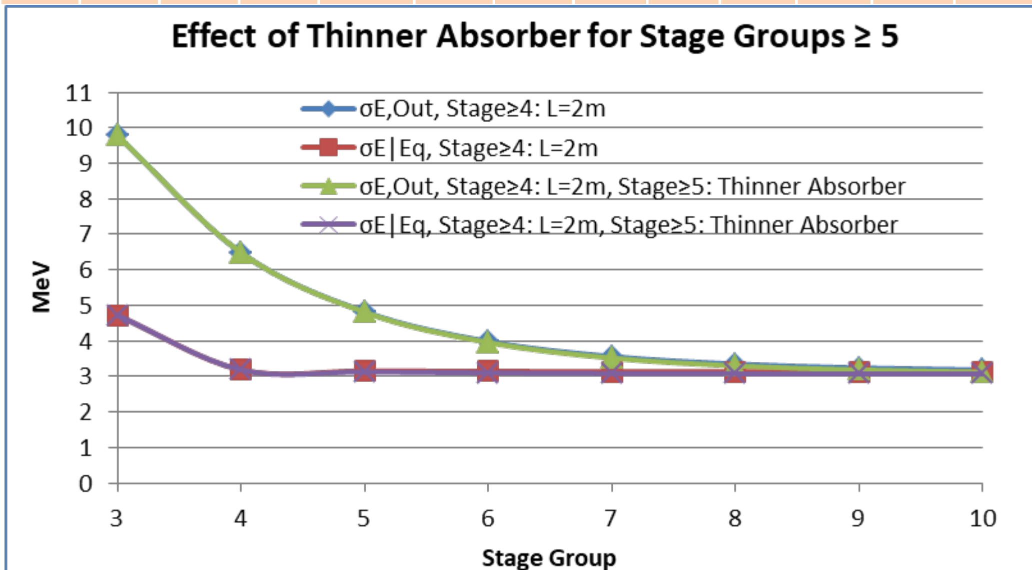

[A] ΔE for energy loss in 4D absorber is not included.

Comments on Modified Enlarged Wedge Geometry

Other configurations can be considered for the modified wedge absorber geometry.

- In the spirit of the Rectilinear channel where the wedge extended beyond the designed muon momenta transverse spatial extent, the wedge likewise can be widened to accommodate effects of the large transverse angles as in the middle cartoon or even the entire transverse extent as in the right cartoon below.
- Particle distributions of momenta and angles from simulations at the wedge exit could help guide the modified wedge design, keeping in mind the longer path lengths traversed by large angled muons.

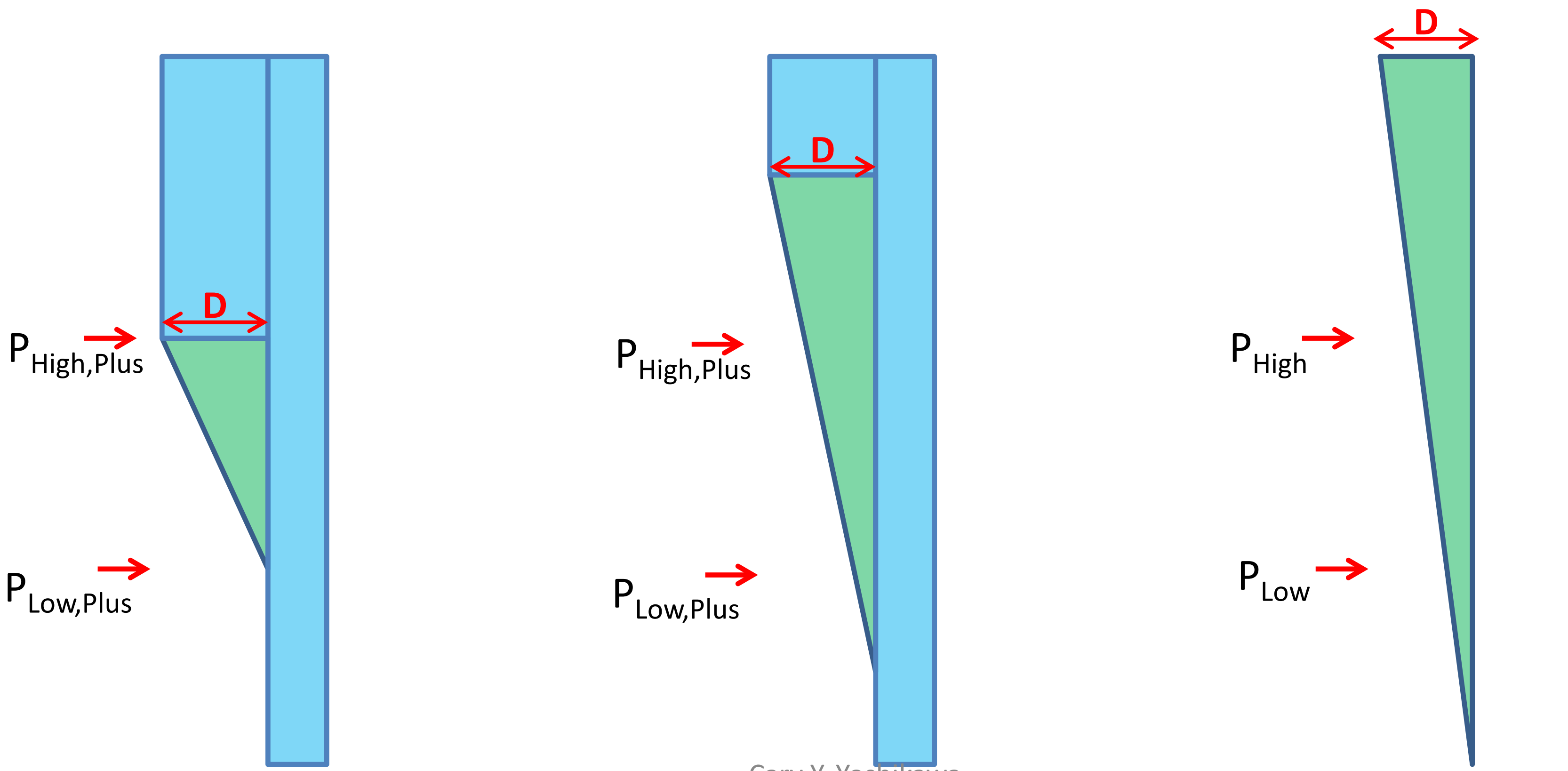

Method to Derive Optimal Absorber Shape

1. With NO absorber in place, create distribution of muons hitting a virtual detector at location of wedge exit.
2. For each muon, extrapolate backwards to the point in location that would result in that particle to lose the amount of energy to end up with P = 200 MeV/c at the virtual detector.
3. A fit to these extrapolated points should yield the optimal front face 2D surface edge of the absorber.
   - The fitting process could have additional weights to account for expected performance of downstream focusing elements. For example, expect co-linear particles to be better focused, so might consider adding a weight of $\cos(\theta)$ or $\cos^2(\theta)$, where θ is the angle with respect to the reference direction.

➢ Note that this method removes the need for the extra D1 (5.35 cm) of LiH absorber, shortening the system and incrementally helping address the large transverse emittance acceptance issue.

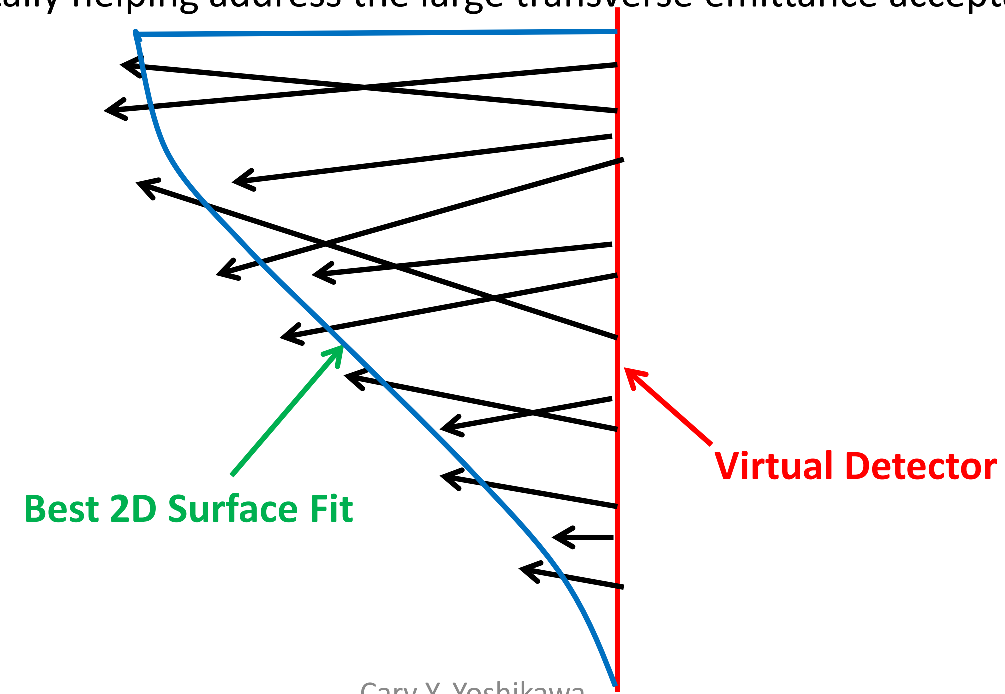

Updated Methods to Cope with Rectilinear Transverse Emittance

- Shorter Configurations
- Contoured Dipole Edges for Focusing in Bend Plane
- Opposing Dipoles of opposite polarities to focus in non-bend plane.
- Possible relaxation of shorter (higher B) configurations to accommodate B=2T.

Shorter Configurations to Address Large Transverse Spread from Rectilinear Channel

Stage	$P_{Low,In}$ (MeV/c)	$P_{High,In}$ (MeV/c)	B (T)	R1 (m) P_{Low}	R2 (m) P_{High}	Dispersion η (m)	Arc Bend θ (degrees)	Wedge Width (m)	Wedge D1 (m)	Wedge D2 (m)	Path Len To Wedge Exit (m) P_{Low}	Path Len To Wedge Exit (m) P_{Mid}	Path Len To Wedge Exit (m) P_{High}	$\sigma_{E,Out}$ (MeV)	$\sigma_{E\|Eq}$ (MeV)	Absorber Width [A] (m)	Absorber Height [B] (m)
Rectilinear						0.006								44.15	39.92		
1	210.00	258.47	1.518	0.461	0.568	0.334	69.436	0.0690	0.0535	0.3269	0.9853	1.0000	1.0147	41.92	5.35	0.4690	0.4000
1	210.00	258.47	2.545	0.275	0.339	0.219	73.339	0.0453	0.0535	0.3269	0.7398	0.7500	0.7602	42.69	6.61	0.3453	0.3000
1	210.00	258.47	3.422	0.205	0.252	0.174	76.325	0.0361	0.0535	0.3269	0.6453	0.6538	0.6623	42.99	7.41	0.2976	0.2615
1	210.00	258.47	7.338	0.095	0.117	0.101	87.289	0.0210	0.0535	0.3269	0.4942	0.5000	0.5058	43.49	9.71	0.2210	0.2000
1	200.00	248.84	1.391	0.479	0.596	0.369	71.720	0.0803	0.0000	0.2712	0.9823	1.0000	1.0177	42.34	5.09	0.4803	0.4000
1	200.00	248.84	2.211	0.301	0.375	0.251	75.073	0.0547	0.0000	0.2712	0.7373	0.7500	0.7627	42.92	6.17	0.3547	0.3000
1	200.00	248.84	4.254	0.157	0.195	0.152	82.191	0.0331	0.0000	0.2712	0.5339	0.5424	0.5509	43.41	7.93	0.2500	0.2170
1	200.00	248.84	5.211	0.128	0.159	0.131	85.107	0.0286	0.0000	0.2712	0.4924	0.5000	0.5076	43.52	8.53	0.2286	0.2000

A: $W_{Absorber} = W_{Wedge} + 2\, L_{pmid}\, [(\Delta Px/2)/Pz]$
B: $H_{Absorber} = 2\, L_{Pmid}\, [(\Delta Px/2)/Pz]$

ΔPx = 80 MeV/c
Pz = 200 MeV/c

	Low	Mid	High
P (MeV/c)	200.00	224.42	248.84
Radius (m)	0.128	0.144	0.159
Arc Bend Angle (°)		85.107	
Wedge Width (m)		0.0286	
Dispersion (m)		0.1313	
Arc Length in Dipole (m)	0.1900	0.2132	0.2364
Distance from Dipole Exit to Wedge Region Entry (m)	0.0311	0.0156	0.0000
Distance in Vac in Wedge Region (m)	0.2712	0.1384	0.0000
Distance in LiH in Wedge Region (m)	0.0000	0.1328	0.2712
Length Dipole Entry to Wedge Exit (m)	0.4924	0.5000	0.5076
Time in Arc (s)	7.17E-10	7.86E-10	8.57E-10
Time from Dipole Exit to Wedge Region Entry (s)	1.17E-10	5.74E-11	0.00E+00
Time in Vac in Wedge Region (s)	1.02E-09	5.10E-10	0.00E+00
Time in LiH in Wedge Region (s)	0.00E+00	4.95E-10	1.00E-09
Time Dipole Entry to Wedge Exit (s)	1.86E-09	1.85E-09	1.86E-09

Contoured Dipole Edges for Focusing in Bend Plane

The edges of the dipole above and below the designed wedge region can be contoured to have particles with Pmax and Pmin of all input angles be parallel upon exit with particles of all momenta that enter the dipole on the reference path (ϕ = 0).

For reference slope m_0, input angle ϕ, and radius R corresponding to the particle's momentum (P = eBR), the x and y coordinates along these edges (in the bending plane) are:

$$x = \pm \frac{m_0 R}{\sqrt{1+m_0^2}} + R\cos\varphi$$

$$y = \pm\sqrt{R^2 - (x - R\cos\varphi)^2} + R\sin\varphi$$

$$\pm\varphi_{max} = \pm\tan^{-1}\left[\frac{\Delta P_x/2}{P_z}\right]$$

$$= \pm\tan^{-1}\frac{40\ MeV/c}{200\ MeV/c} = \pm 11.3°$$

Shown at right is a contoured dipole for the configuration highlighted on the previous slide with L = 0.5 m and D1 = 0 m.

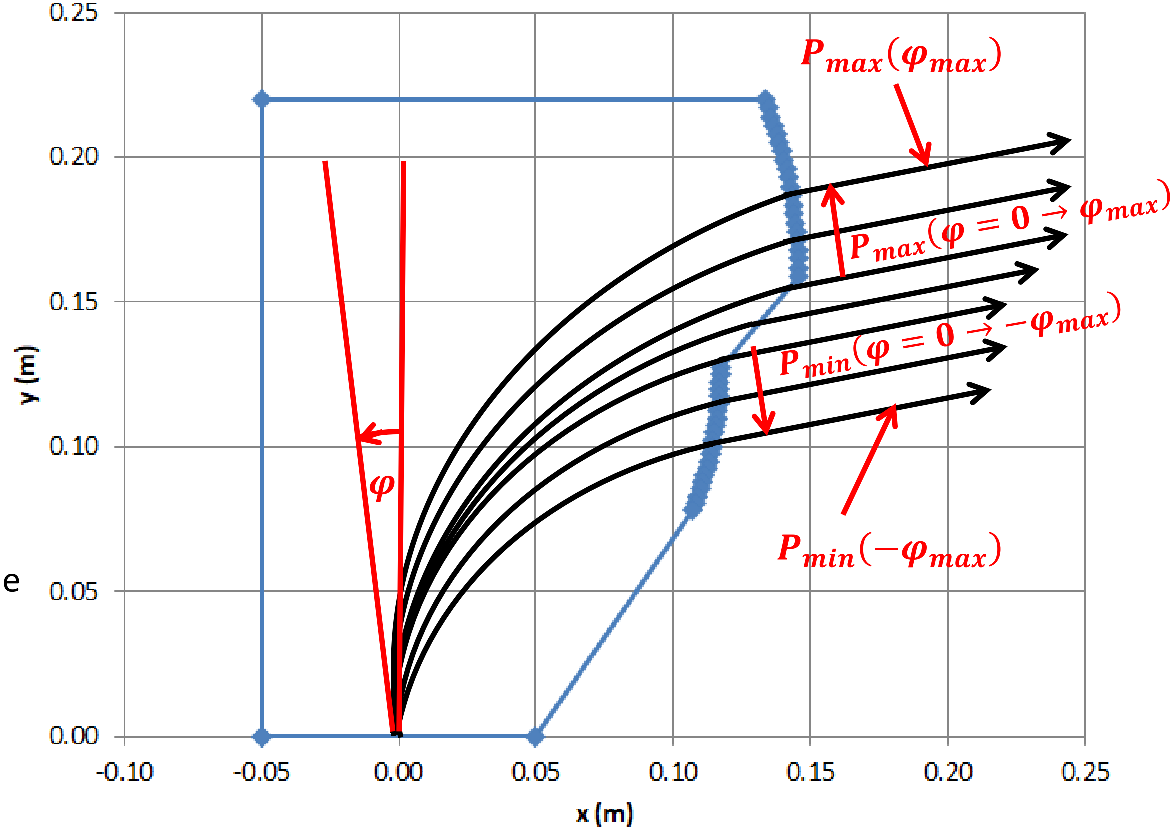

Stage	$P_{Low,In}$ (MeV/c)	$P_{High,In}$ (MeV/c)	B (T)	R1 (m) P_{Low}	R2 (m) P_{High}	Dispersion η (m)	Arc Bend θ (degrees)	Wedge Width (m)	Wedge D1 (m)	Wedge D2 (m)	Path Len To Wedge Exit (m) P_{Low}	Path Len To Wedge Exit (m) P_{Mid}	Path Len To Wedge Exit (m) P_{High}	$\sigma_{E,Out}$ (MeV)	$\sigma_{E\|Eq}$ (MeV)	Absorber Width [A] (m)	Absorber Height [B] (m)
Rectilinear						0.006								44.15	39.92		
1	210.00	258.47	1.518	0.461	0.568	0.334	69.436	0.0690	0.0535	0.3269	0.9853	1.0000	1.0147	41.92	5.35	0.4690	0.4000
1	210.00	258.47	2.545	0.275	0.339	0.219	73.339	0.0453	0.0535	0.3269	0.7398	0.7500	0.7602	42.69	6.61	0.3453	0.3000
1	210.00	258.47	3.422	0.205	0.252	0.174	76.325	0.0361	0.0535	0.3269	0.6453	0.6538	0.6623	42.99	7.41	0.2976	0.2615
1	210.00	258.47	7.338	0.095	0.117	0.101	87.289	0.0210	0.0535	0.3269	0.4942	0.5000	0.5058	43.49	9.71	0.2210	0.2000
1	200.00	248.84	1.391	0.479	0.596	0.369	71.720	0.0803	0.0000	0.2712	0.9823	1.0000	1.0177	42.34	5.09	0.4803	0.4000
1	200.00	248.84	2.211	0.301	0.375	0.251	75.073	0.0547	0.0000	0.2712	0.7373	0.7500	0.7627	42.92	6.17	0.3547	0.3000
1	200.00	248.84	4.254	0.157	0.195	0.152	82.191	0.0331	0.0000	0.2712	0.5339	0.5424	0.5509	43.41	7.93	0.2500	0.2170
1	200.00	248.84	5.211	0.128	0.159	0.131	85.107	0.0286	0.0000	0.2712	0.4924	0.5000	0.5076	43.52	8.53	0.2286	0.2000

A: $W_{Absorber} = W_{Wedge} + 2\, L_{Pmid}\, [(\Delta Px/2)/Pz]$

B: $H_{Absorber} = 2\, L_{Pmid}\, [(\Delta Px/2)/Pz]$

$\Delta Px = 80$ MeV/c

$Pz = 200$ MeV/c

Reduction in bending plane compared to straight drift:

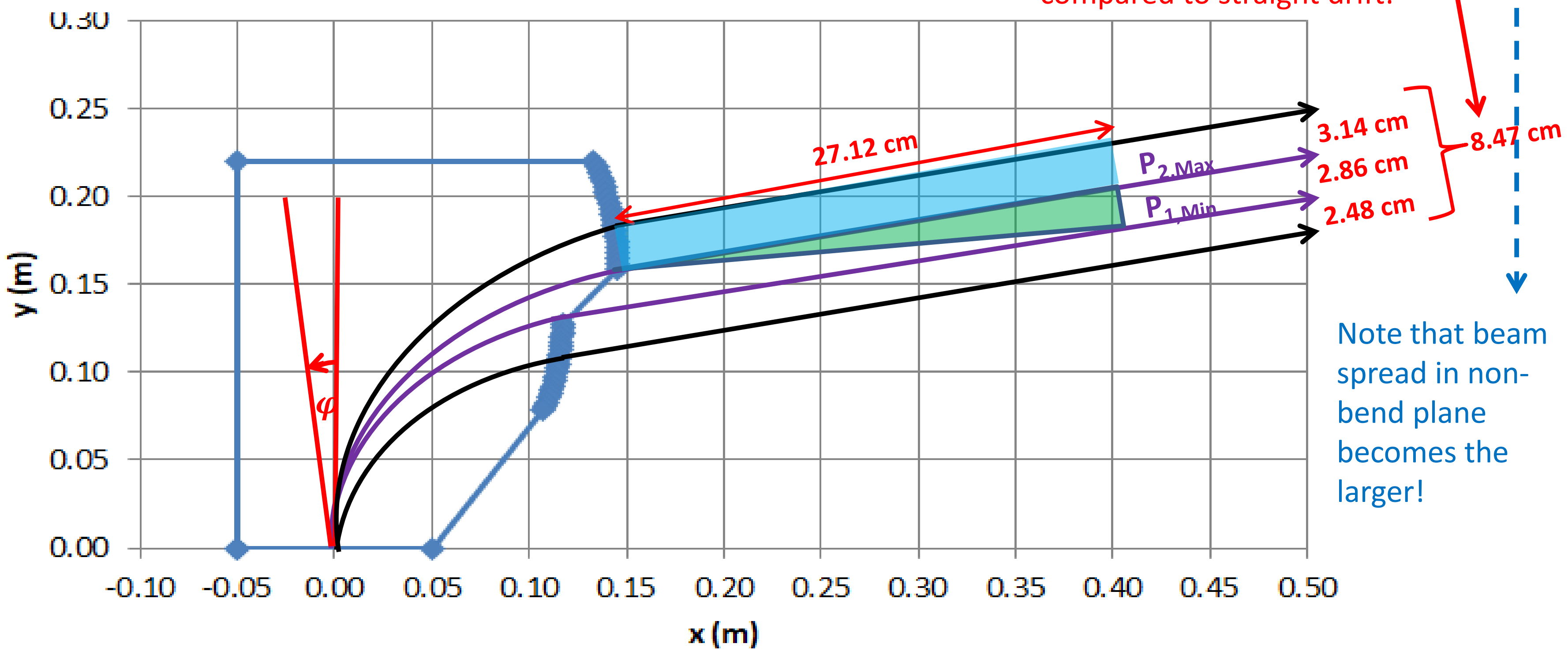

Once an optimized absorber shape is derived from simulations described earlier, $L_{1,\text{Wedge Area,Vac}}$ and $L_{2,\text{Wedge Area,Vac}}$ can be determined and the isochronous condition can be reapplied using an updated formula:

$$\left[\frac{R_2}{v_2} - \frac{R_1}{v_1}\right]\theta - \frac{(R_2 - R_1)}{v_1}\sin\theta + \frac{L_{2,WedgeArea,Vac}}{v_2} + t_{2,LiH} - \frac{L_{1,WedgeArea,Vac}}{v_1} - t_{1,LiH} = 0$$

The isochronous condition will yield a configuration (θ) that hopefully is not too different that becomes the basis for simulations to derive a re-optimized absorber shape. The simulations for the re-optimized absorber would involve a virtual detector located D (27.12 cm below) distance downstream from the dipole exit of a muon with max ϕ and $P_{2,\text{Max}}$. This re-optimized absorber will yield modified values for $L_{1,\text{Wedge Area,Vac}}$ and $L_{2,\text{Wedge Area,Vac}}$ that would be subject to reapplication of the isochronous condition. Hopefully, this iterative procedure converges quickly and ultimately will rest at the design tolerance for isochronicity out of the absorber.

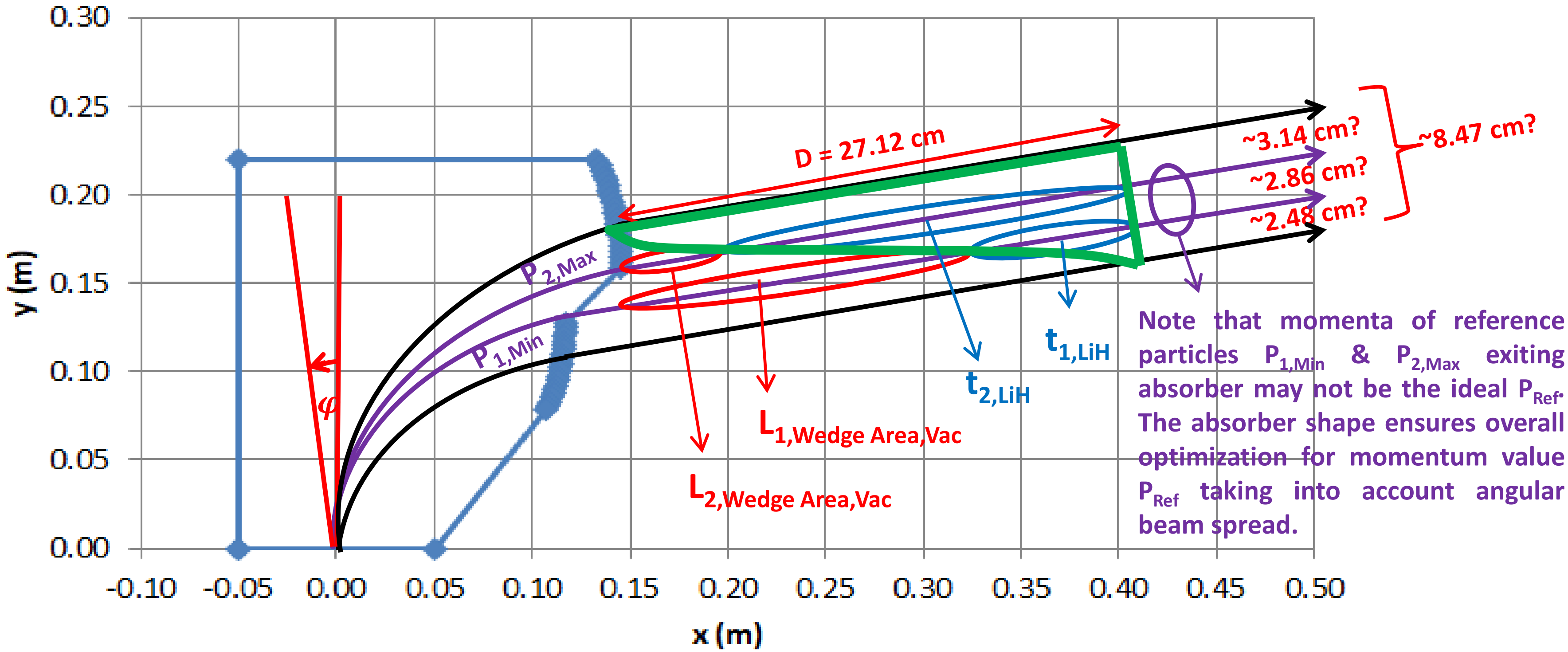

Note that momenta of reference particles $P_{1,\text{Min}}$ & $P_{2,\text{Max}}$ exiting absorber may not be the ideal P_{Ref}. The absorber shape ensures overall optimization for momentum value P_{Ref} taking into account angular beam spread.

Addressing Vertical Spread

To address the vertical spread of the beam, edges of the dipole parallel to the enveloping particle trajectories are contoured to accommodate coils that provide the focusing B fields. Below shows contours for $2\phi_{max}$, but this tolerance can be tightened (say to 1.5 ϕ_{max}) if needed to provide desired B fields.

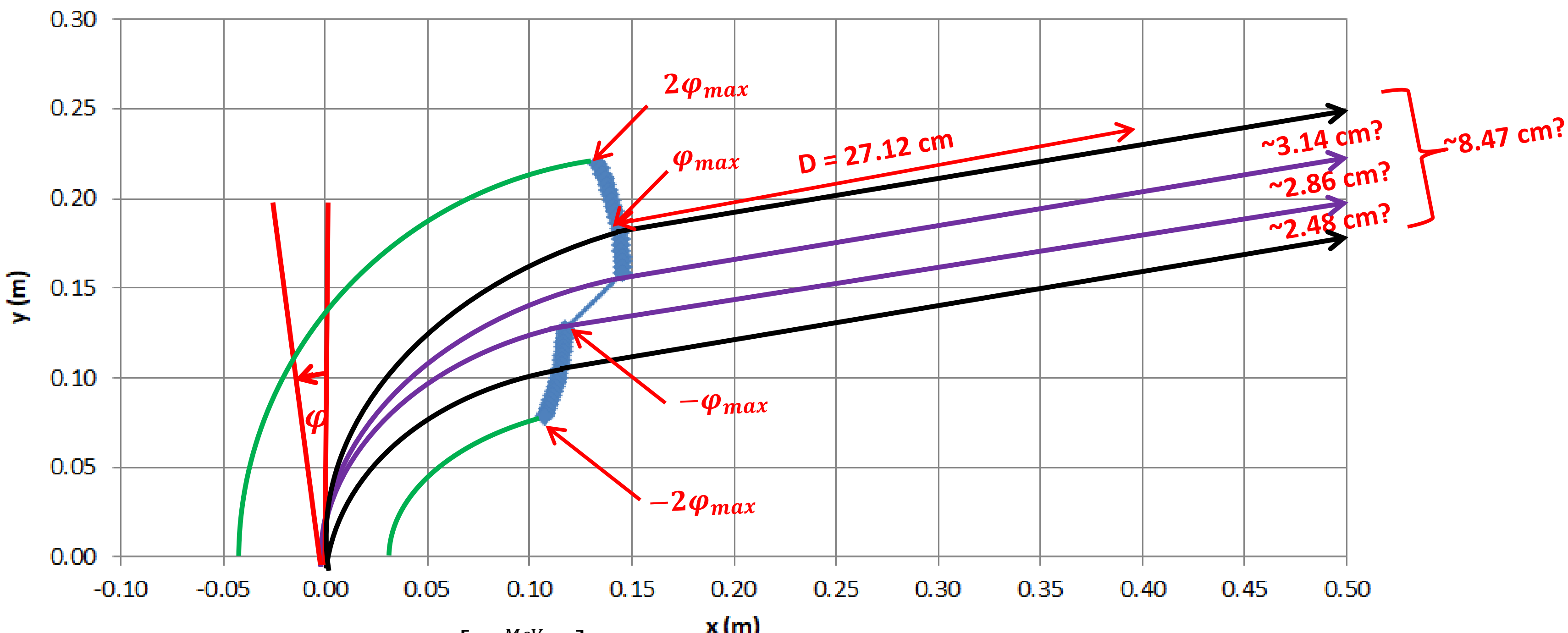

$$\pm\varphi_{max} = \pm\tan^{-1}\left[\frac{(\Delta P_{x,y})/2}{P_z}\right] = \pm\tan^{-1}\left[\frac{(80\frac{MeV}{c})/2}{200\,\frac{MeV}{c}}\right] = \pm 11.3^{o}$$

Addressing Vertical Spread

Coils of opposing polarity are added transverse to the dipole field, creating a B field in the radial direction that varies with the vertical position, being zero in the mid-plane. To estimate the effect of the two opposing coils, we assume a linear gradient away from the mid-plane and that appropriate placement of the coils might maintain sufficient gradient throughout the active volume.

- A gradient of -40.75 T/m provides B_r = -0.986 T at y = 2.4 cm and is able to rotate a muon with P_y = 40 MeV/c at dipole entry to be parallel with the reference upon exit.

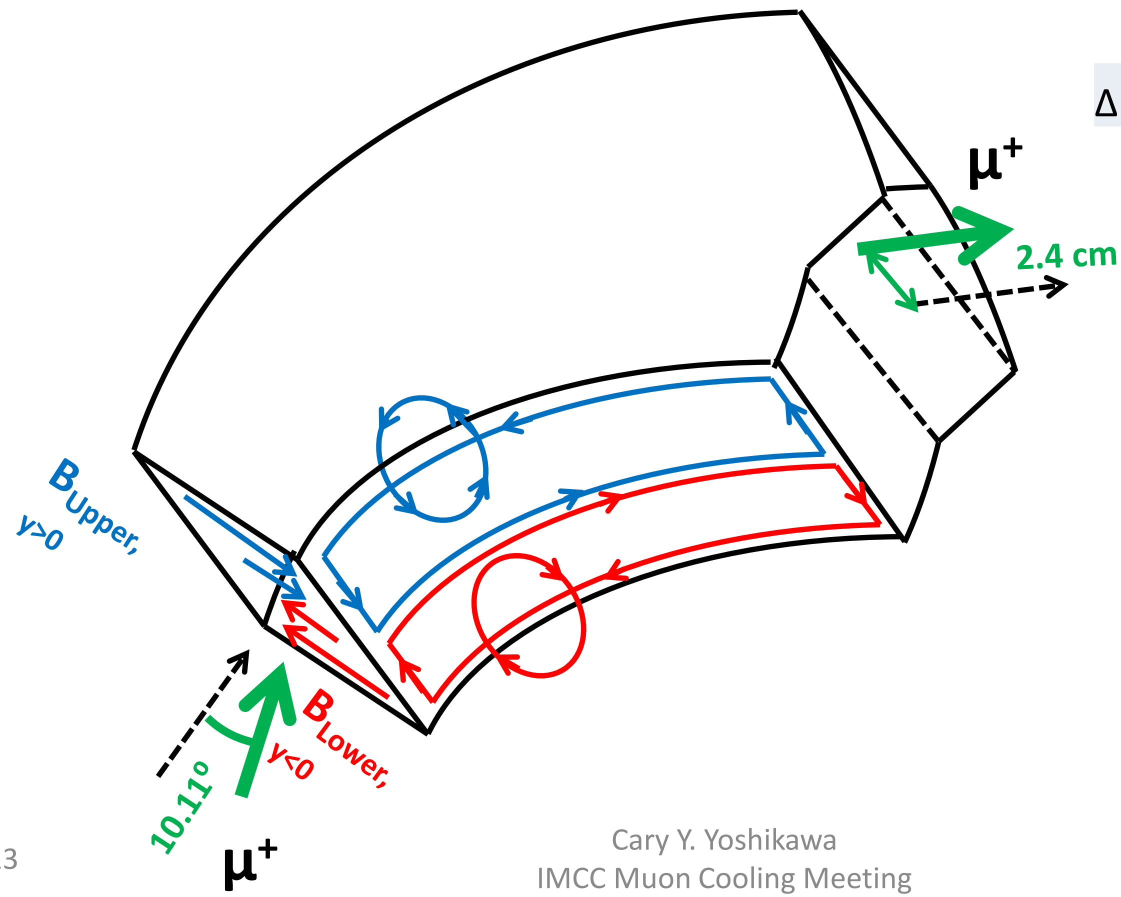

$\Delta B_r/\Delta y$ (T/m)	- 40.75

$P_{z,In}$ (MeV/c)	224.42
$P_{y,In}$ (MeV/c)	40.00
y_{In} (m)	0.00
θ_{In} (deg)	10.11
Arc Length in Dipole (m)	0.213
$B_r(y)$ (T)	- 0.986
$P_{z,Out}$ (MeV/c)	227.98
$P_{y,Out}$ (MeV/c)	0.00
y_{Out} (m)	0.024
θ_{Out} (deg)	0.00

Revisit Shorter Configurations to Address Large Transverse Spread from Rectilinear Channel with B=2T

Stage	$P_{Low,In}$ (MeV/c)	$P_{High,In}$ (MeV/c)	B (T)	R1 (m) P_{Low}	R2 (m) P_{High}	Dispersion η (m)	Arc Bend θ (degrees)	Wedge Width (m)	Wedge D1 (m)	Wedge D2 (m)	Path Len To Wedge Exit (m) P_{Low}	Path Len To Wedge Exit (m) P_{Mid}	Path Len To Wedge Exit (m) P_{High}	$\sigma_{E,Out}$ (MeV)	$\sigma_{E\|Eq}$ (MeV)	Absorber Width [A] (m)	Absorber Height [B] (m)
Rectilinear						0.006								44.15	39.92		
1	210.00	258.47	1.518	0.461	0.568	0.334	69.436	0.0690	0.0535	0.3269	0.9853	1.0000	1.0147	41.92	5.35	0.4690	0.4000
1	210.00	258.47	2.545	0.275	0.339	0.219	73.339	0.0453	0.0535	0.3269	0.7398	0.7500	0.7602	42.69	6.61	0.3453	0.3000
1	210.00	258.47	3.422	0.205	0.252	0.174	76.325	0.0361	0.0535	0.3269	0.6453	0.6538	0.6623	42.99	7.41	0.2976	0.2615
1	210.00	258.47	7.338	0.095	0.117	0.101	87.289	0.0210	0.0535	0.3269	0.4942	0.5000	0.5058	43.49	9.71	0.2210	0.2000
1	200.00	248.84	1.391	0.479	0.596	0.369	71.720	0.0803	0.0000	0.2712	0.9823	1.0000	1.0177	42.34	5.09	0.4803	0.4000
1	200.00	248.84	2.000	0.333	0.415	0.272	74.243	0.0593	0.0000	0.2712	0.7815	0.7950	0.8086	42.81	5.92	0.3773	0.3180
1	200.00	248.84	2.211	0.301	0.375	0.251	75.073	0.0547	0.0000	0.2712	0.7373	0.7500	0.7627	42.92	6.17	0.3547	0.3000
1	200.00	248.84	4.254	0.157	0.195	0.152	82.191	0.0331	0.0000	0.2712	0.5339	0.5424	0.5509	43.41	7.93	0.2500	0.2170
1	200.00	248.84	5.211	0.128	0.159	0.131	85.107	0.0286	0.0000	0.2712	0.4924	0.5000	0.5076	43.52	8.53	0.2286	0.2000

A: $W_{Absorber} = W_{Wedge} + 2\ L_{pmid}\ [(\Delta Px/2)/Pz]$
B: $H_{Absorber} = 2\ L_{pmid}\ [(\Delta Px/2)/Pz]$

$\Delta Px = 80$ MeV/c
$Pz = 200$ MeV/c

	Low	Mid	High
P (MeV/c)	200.00	224.42	248.84
Radius (m)	0.333	0.374	0.415
Arc Bend Angle (^{o})		74.243	
Wedge Width (m)		0.0593	
Dispersion (m)		0.2725	
Arc Length in Dipole (m)	0.4319	0.4847	0.5374
Distance from Dipole Exit to Wedge Region Entry (m)	0.0783	0.0392	0.0000
Distance in Vac in Wedge Region (m)	0.2712	0.1384	0.0000
Distance in LiH in Wedge Region (m)	0.0000	0.1328	0.2712
Length Dipole Entry to Wedge Exit (m)	0.7815	0.7950	0.8086
Time in Arc (s)	1.63E-09	1.79E-09	1.95E-09
Time from Dipole Exit to Wedge Region Entry (s)	2.96E-10	1.44E-10	0.00E+00
Time in Vac in Wedge Region (s)	1.02E-09	5.10E-10	0.00E+00
Time in LiH in Wedge Region (s)	0.00E+00	4.95E-10	1.00E-09
Time Dipole Entry to Wedge Exit (s)	2.95E-09	2.94E-09	2.95E-09

Contoured Dipole Edges for Particles with P_{max} & P_{min} of All Input Angles to be Parallel at Exit with Particles of All Momenta Entering Dipole on Reference Path

The edges of the dipole above and below the designed wedge region can be contoured to have particles with Pmax and Pmin of all input angles be parallel upon exit with particles of all momenta that enter the dipole on the reference path (ϕ = 0).

For reference slope m_0, input angle ϕ, and radius R corresponding to the particle's momentum (P = eBR), the x and y coordinates along these edges are:

$$x = \pm \frac{m_0 R}{\sqrt{1 + m_0^2}} + R\cos\varphi$$

$$y = \pm\sqrt{R^2 - (x - R\cos\varphi)^2} + R\sin\varphi$$

$$\pm\varphi_{max} = \pm\tan^{-1}\left[\frac{\Delta P_x/2}{P_z}\right]$$

$$= \pm\tan^{-1}\frac{40\ MeV/c}{200\ MeV/c} = \pm 11.3°$$

Shown at right is a contoured dipole for the configuration highlighted on the previous slide with **B = 2 T** and L = 0.795 m.

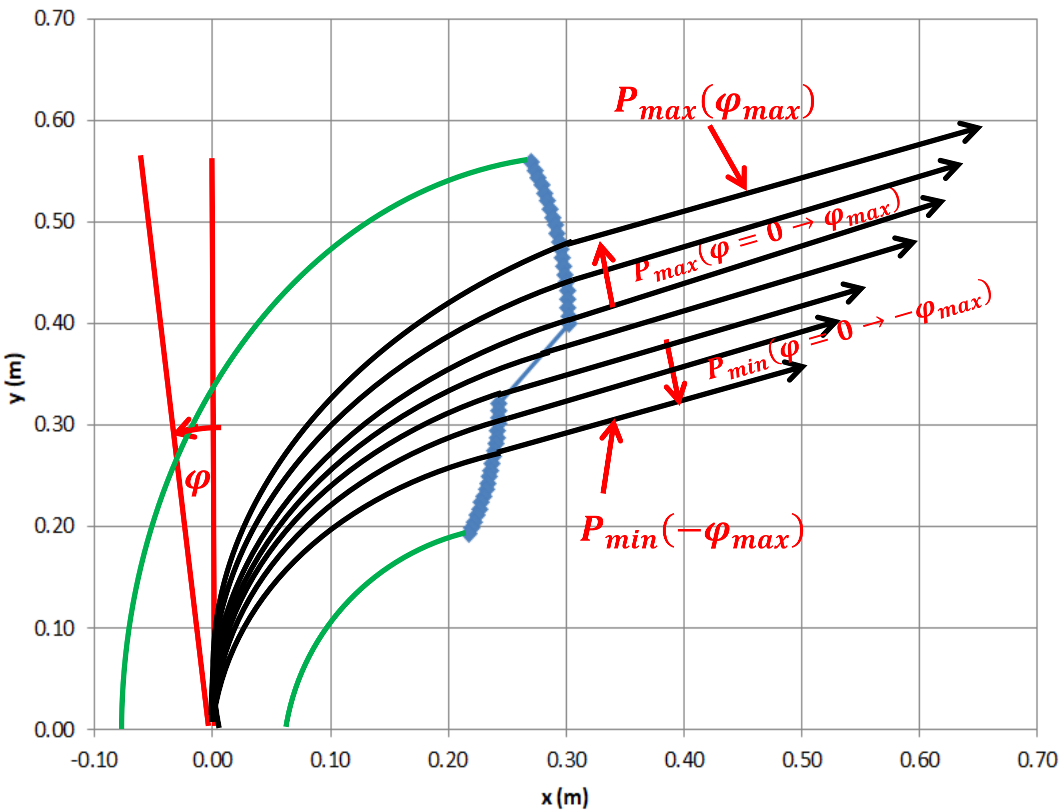

Stage	$P_{Low,In}$ (MeV/c)	$P_{High,In}$ (MeV/c)	B (T)	R1 (m) P_{Low}	R2 (m) P_{High}	Dispersion η (m)	Arc Bend θ (degrees)	Wedge Width (m)	Wedge D1 (m)	Wedge D2 (m)	Path Len To Wedge Exit (m) P_{Low}	Path Len To Wedge Exit (m) P_{Mid}	Path Len To Wedge Exit (m) P_{High}	$\sigma_{E,Out}$ (MeV)	$\sigma_{E\|Eq}$ (MeV)	Absorber Width [A] (m)	Absorber Height [B] (m)
Rectilinear						0.006								44.15	39.92		
1	210.00	258.47	1.518	0.461	0.568	0.334	69.436	0.0690	0.0535	0.3269	0.9853	1.0000	1.0147	41.92	5.35	0.4690	0.4000
1	210.00	258.47	2.545	0.275	0.339	0.219	73.339	0.0453	0.0535	0.3269	0.7398	0.7500	0.7602	42.69	6.61	0.3453	0.3000
1	210.00	258.47	3.422	0.205	0.252	0.174	76.325	0.0361	0.0535	0.3269	0.6453	0.6538	0.6623	42.99	7.41	0.2976	0.2615
1	210.00	258.47	7.338	0.095	0.117	0.101	87.289	0.0210	0.0535	0.3269	0.4942	0.5000	0.5058	43.49	9.71	0.2210	0.2000
1	200.00	248.84	1.391	0.479	0.596	0.369	71.720	0.0803	0.0000	0.2712	0.9823	1.0000	1.0177	42.34	5.09	0.4803	0.4000
1	200.00	248.84	2.000	0.333	0.415	0.272	74.243	0.0593	0.0000	0.2712	0.7815	0.7950	0.8086	42.81	5.92	0.3773	0.3180
1	200.00	248.84	2.211	0.301	0.375	0.251	75.073	0.0547	0.0000	0.2712	0.7373	0.7500	0.7627	42.92	6.17	0.3547	0.3000
1	200.00	248.84	4.254	0.157	0.195	0.152	82.191	0.0331	0.0000	0.2712	0.5339	0.5424	0.5509	43.41	7.93	0.2500	0.2170
1	200.00	248.84	5.211	0.128	0.159	0.131	85.107	0.0286	0.0000	0.2712	0.4924	0.5000	0.5076	43.52	8.53	0.2286	0.2000

A: $W_{Absorber} = W_{Wedge} + 2\, L_{Pmid}\, [(\Delta Px/2)/Pz]$

B: $H_{Absorber} = 2\, L_{Pmid}\, [(\Delta Px/2)/Pz]$

$\Delta Px = 80$ MeV/c

$Pz = 200$ MeV/c

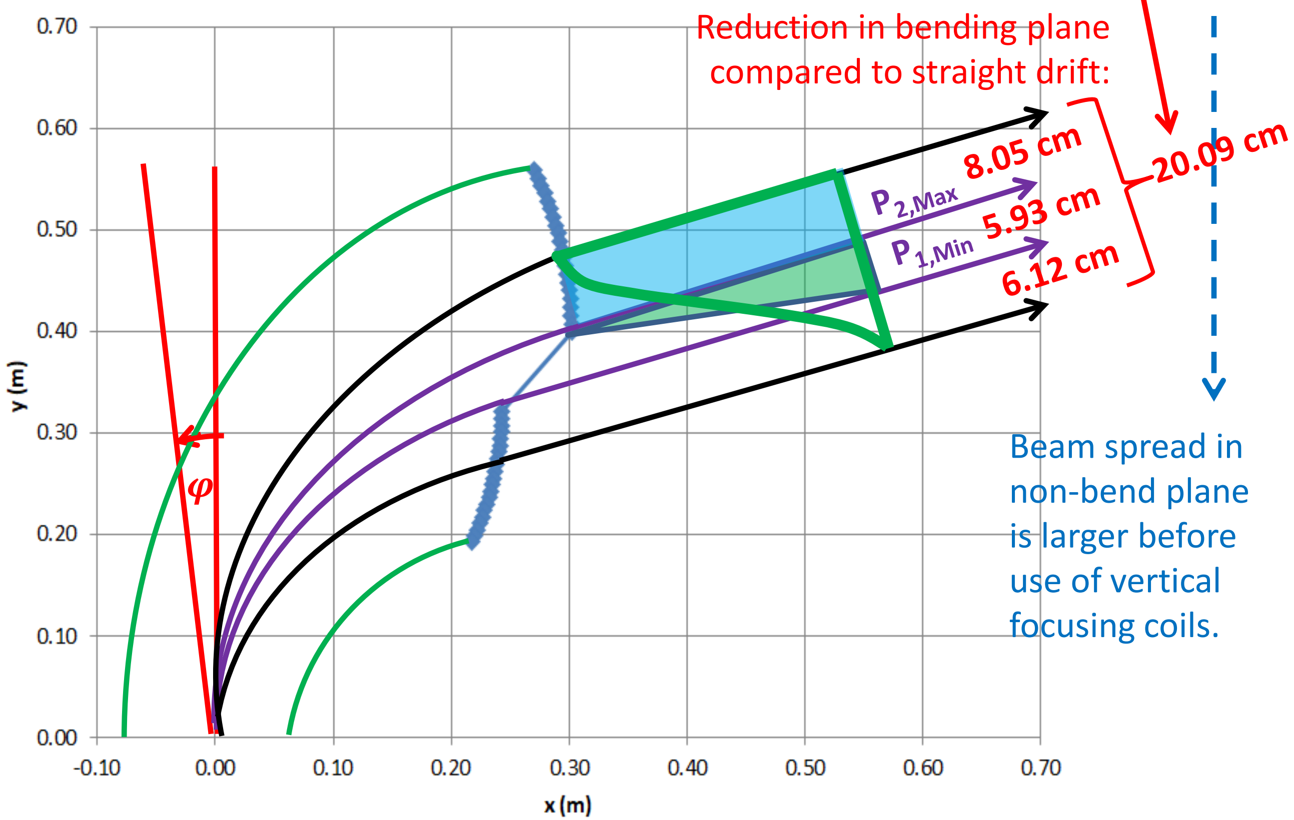

Addressing Vertical Spread

- A gradient of -7.91 T/m provides B_r = -0.433 T at y = 5.5 cm and is able to rotate a muon with P_y = 40 MeV/c at dipole entry to be parallel with the reference upon exit.
- A muon entering the dipole at y= 1 cm with Py = 0 & Pz = 224.42 MeV/c experiences B_r = -0.079 T at entry and exits the dipole at y = ~0 (5.6E-6m) with Py = -7.31 MeV/c & Pz = 224.30 MeV/c, resulting in θ_{Out} = -1.87°.

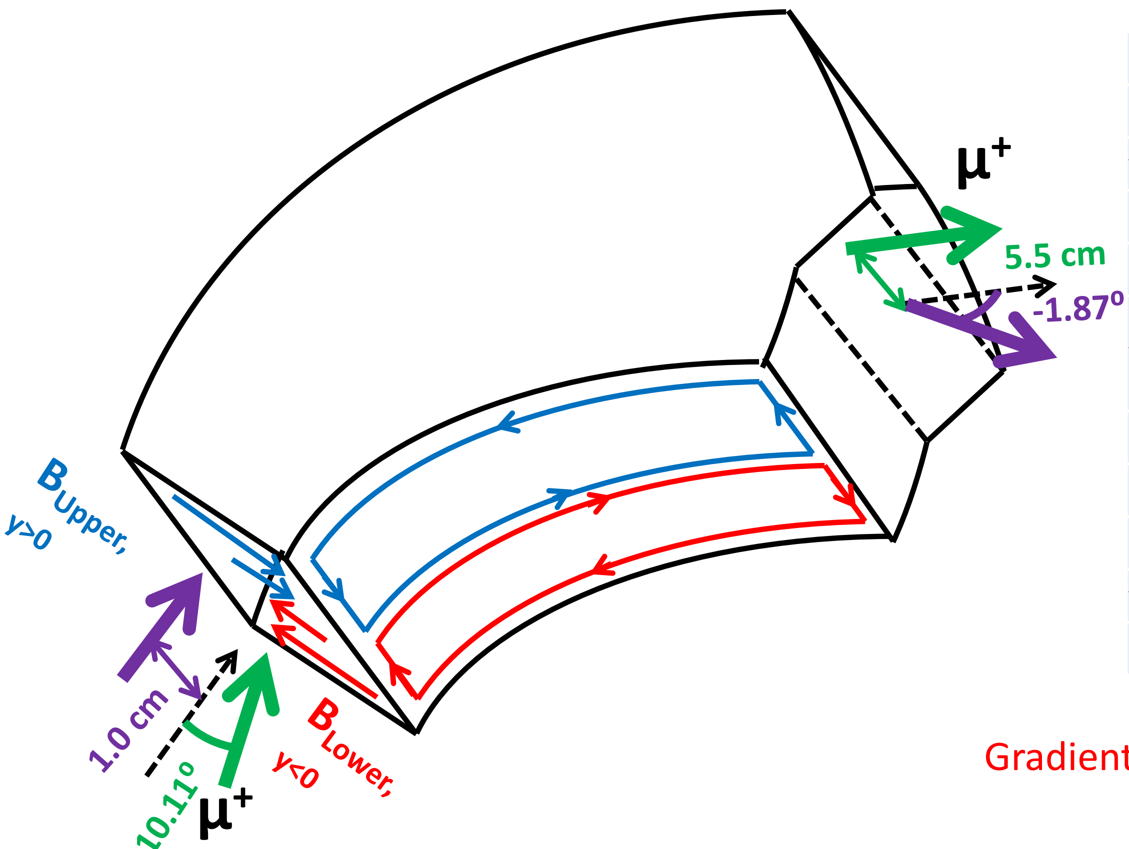

$\Delta B_r/\Delta y$ (T/m)	- 7.91	
$P_{z,In}$ (MeV/c)	224.42	224.42
$P_{y,In}$ (MeV/c)	40.00	0.00
y_{In} (m)	0.00	0.010
θ_{In} (deg)	10.11	0.000
$B_{r,In}(y)$ (T)	0.00	-0.079
Arc Length in Dipole (m)	0.485	
$B_{r,Out}$ (y) (T)	-0.433	0.000
$P_{z,Out}$ (MeV/c)	227.97	224.30
$P_{y,Out}$ (MeV/c)	0.00	-7.31
y_{Out} (m)	0.055	0.000
θ_{Out} (deg)	0.00	-1.87

Gradient tuned to achieve θ_{Out} = 0 at exit.

Addressing Vertical Spread

- A gradient of -7.91 T/m provides B_r = -0.433 T at y = 5.5 cm and is able to rotate a muon with P_y = 40 MeV/c at dipole entry to be parallel with the reference upon exit.
- A muon entering the dipole at y= 1 cm with Py = 0 & Pz = 224.42 MeV/c experiences B_r = -0.079 T at entry and exits the dipole at y = ~0 (5.6E-6m) with Py = -7.31 MeV/c & Pz = 224.30 MeV/c, resulting in θ_{Out} = -1.87°.

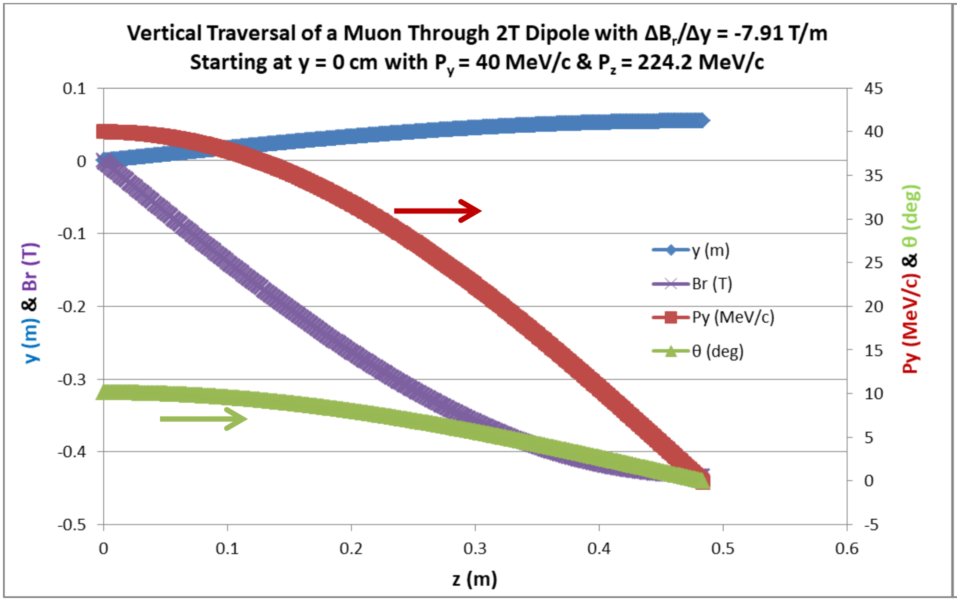

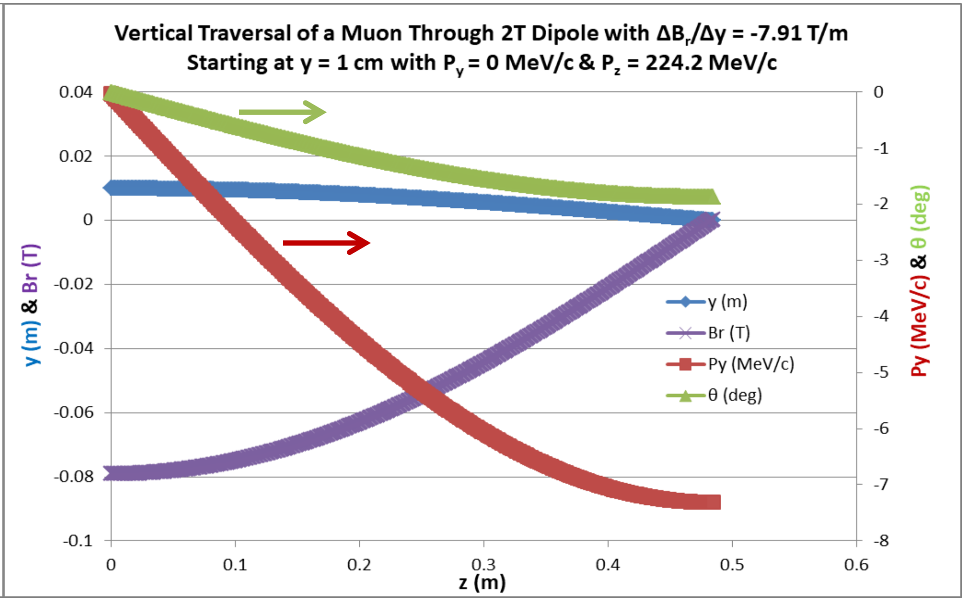

Addressing Vertical Spread

Biot-Savart calculations were performed on a simplified geometry using straight segments instead of the curved to estimate what may be possible.

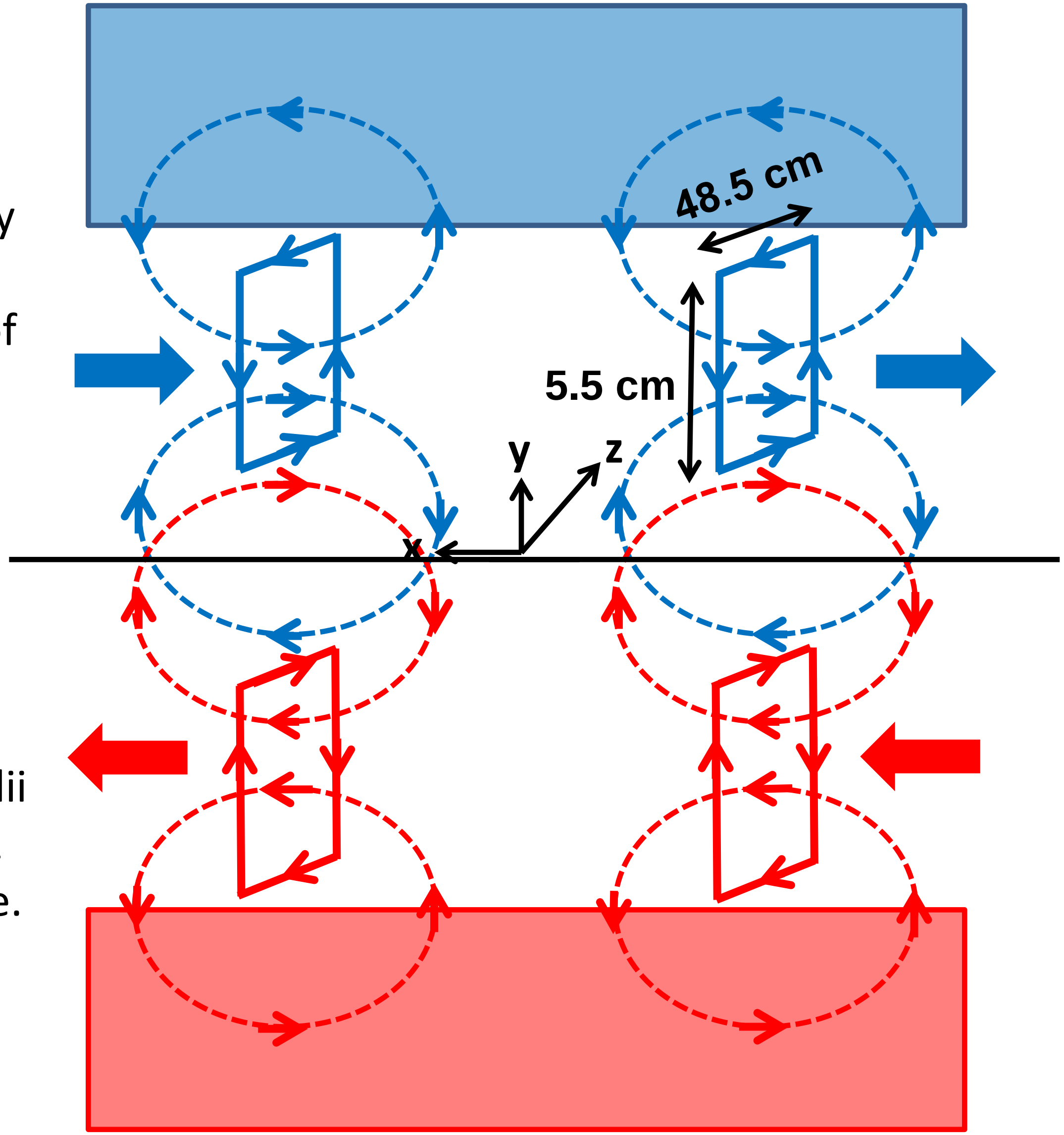

It may be best to have the distance between coils at inner and outer radii be constant along z as much as possible.

Addressing Vertical Spread

B_x contribution from vertical current segments at the entrance and exit of dipole is less than 0.6% of that from current segments in the dipole parallel to the beam and have been ignored in the calculations for the current.

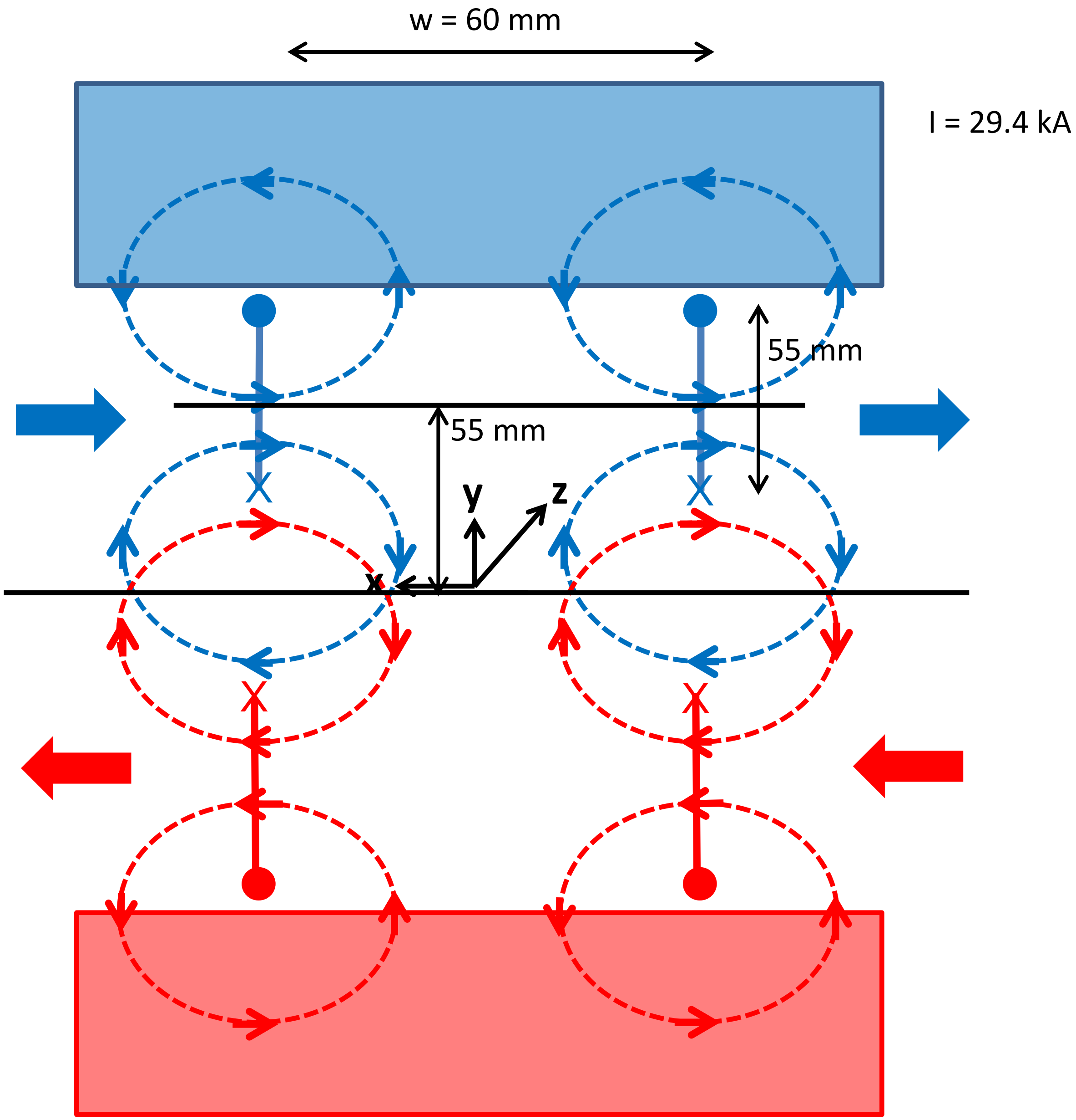

Addressing Vertical Spread

Current density of 220 A/mm² from Rectilinear cell B8 in presentation by Siara Fabbri & Jonathan Pavan at the 5/15/23 IMCC Accelerator Design Meeting.

$I = 29.4$ kA
$J = 220$ A/mm²
$\sigma = 134$ mm²
$L_x = 10$ mm, $L_y = 13.4$ mm?
$L_x = L_y = 11.6$ mm?

B_x contribution from vertical current segments at the entrance and exit of dipole is less than 0.6% of that from current segments in the dipole parallel to the beam and have been ignored in the calculations for the current.

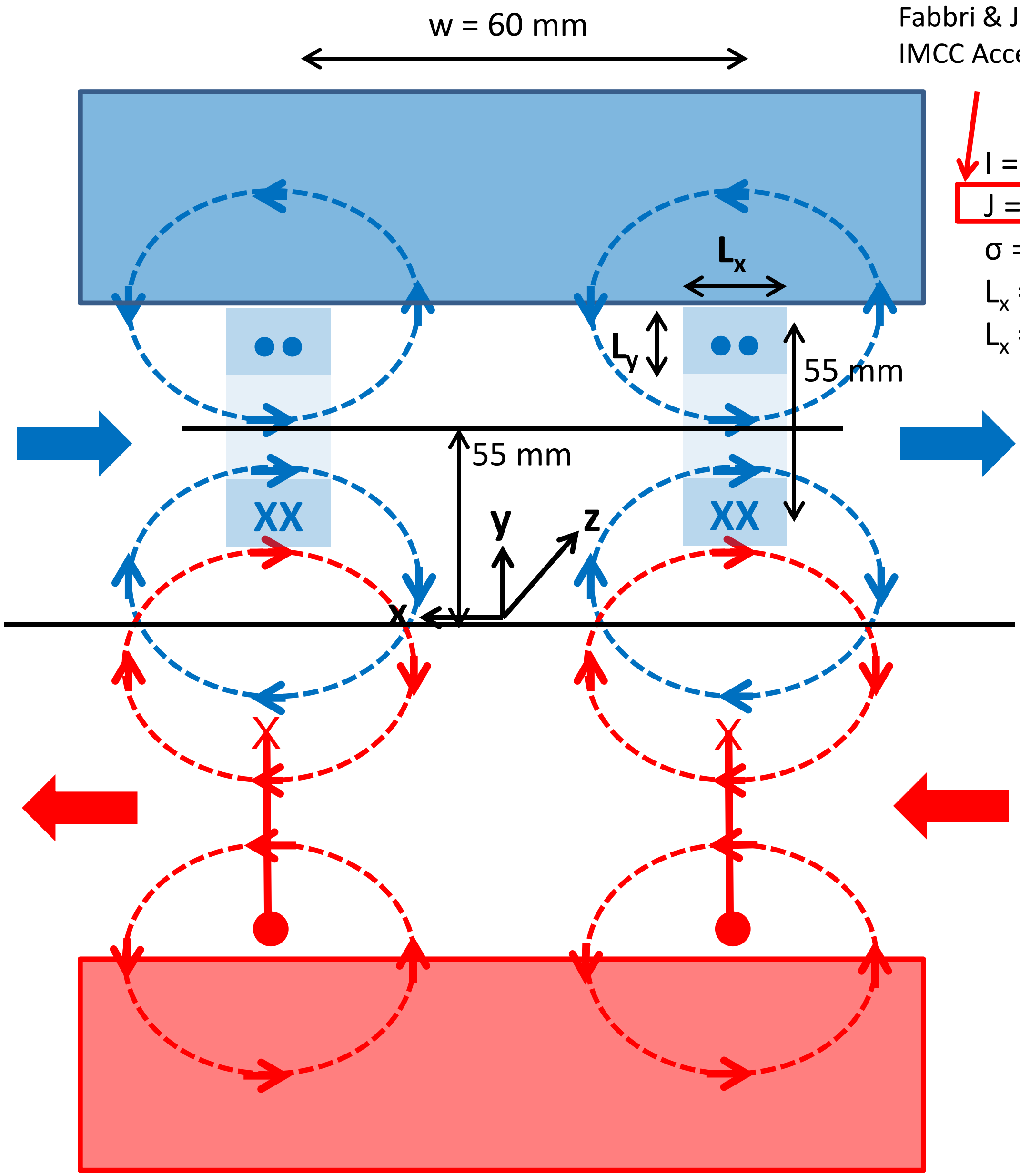

Addressing Vertical Spread

B_x contribution from vertical current segments at the entrance and exit of dipole is ~3% of that from current segments in the dipole parallel to the beam and have been ignored in the calculations for the current.

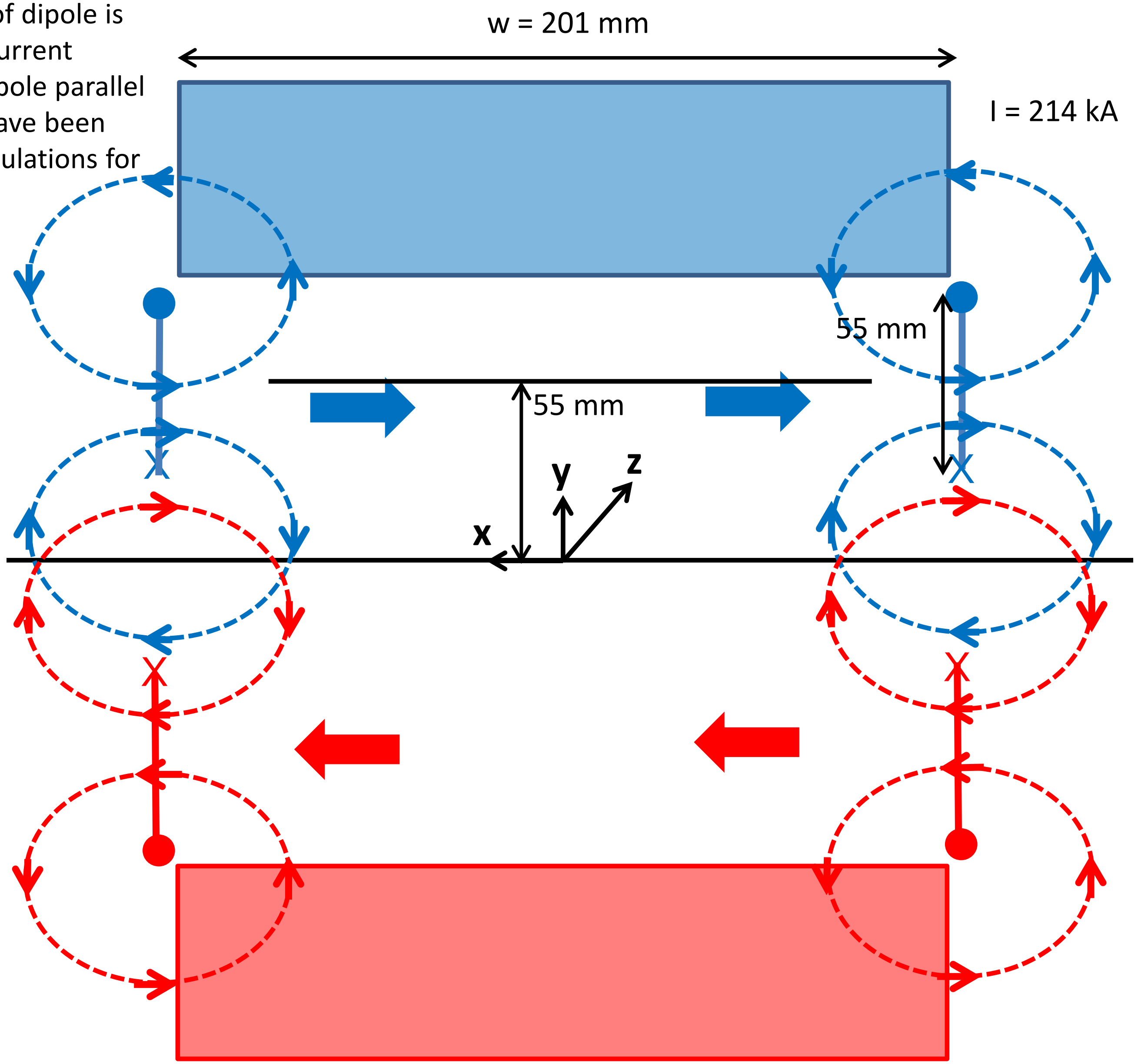

Addressing Vertical Spread

B_x contribution from vertical current segments at the entrance and exit of dipole is ~3% of that from current segments in the dipole parallel to the beam and have been ignored in the calculations for the current.

I = 214 kA
J = 220 A/mm^2
σ = 975 mm^2
L_x = 10 mm, L_y = 97.5 mm?

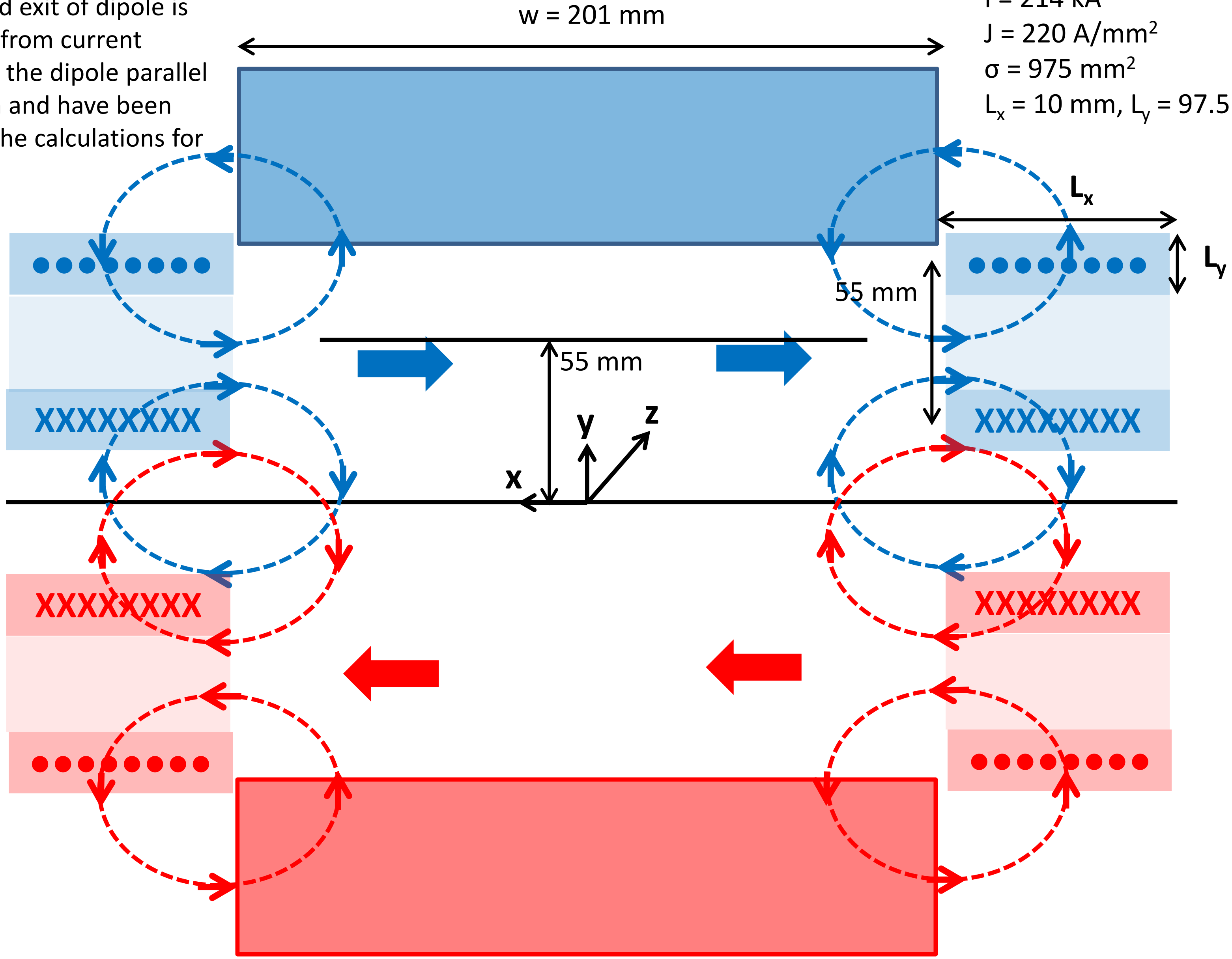

Addressing Vertical Spread

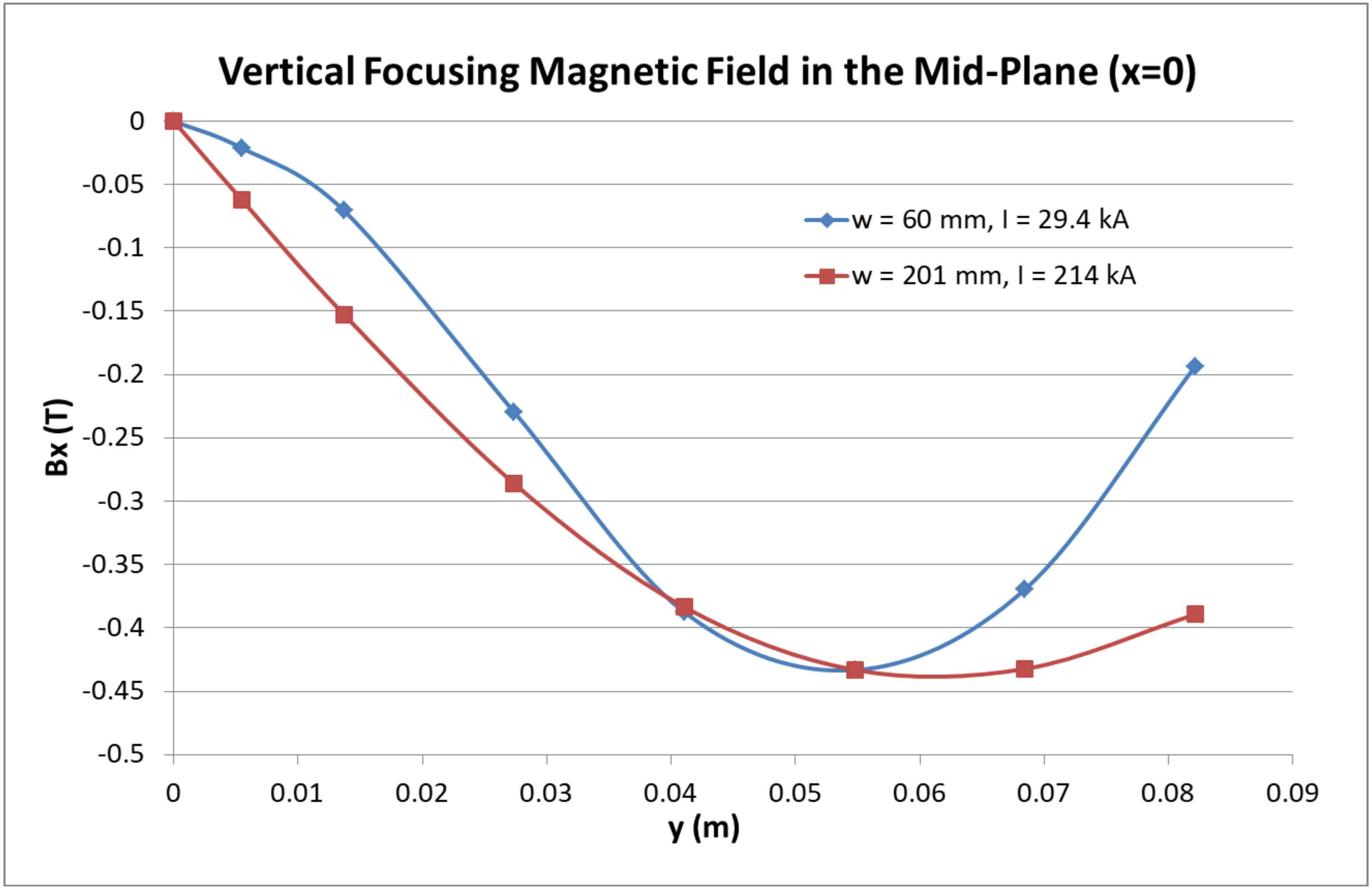

The configuration with the coils at the edges (w = 201 mm) provides a more linear gradient and suffers less fall off at higher y values, but requires more current. However, this geometry allows more space to achieve the desired current.

Stage 1 Comparison Between Configurations with L = 0.5m vs. B = 2 T

$P_{Low,In}$ (MeV/c)	$P_{High,In}$ (MeV/c)	B (T)	R1 (m) P_{Low}	R2 (m) P_{High}	Dispersion η (m)	Arc Bend θ (deg)	Wedge Width (m)	Wedge D1 (m)	Wedge D2 (m)	Path Len To Wedge Exit (m) P_{Low}	Path Len To Wedge Exit (m) P_{Mid}	Path Len To Wedge Exit (m) P_{High}	**Updated** Absorber Width (m)	**Updated** Absorber Height (m)
200.00	248.84	2.00	0.333	0.415	0.272	74.243	0.0593	0.0000	0.2712	0.7815	0.7950	0.8086	0.2009	0.1097
200.00	248.84	5.21	0.128	0.159	0.131	85.107	0.0286	0.0000	0.2712	0.4924	0.5000	0.5076	0.0847	0.0484

Summary

A design framework and concepts for 6D cooling beyond that of the Rectilinear channel have been presented that address emittances in each dimension.

- To minimize the energy spread σ_E, large dispersion is exploited to minimize its equilibrium:

$$\sigma_E|_{Eq} = \beta\gamma(r_e m_e c^2)\sqrt{\frac{2\pi n_e\left(1-\frac{\beta^2}{2}\right)E}{\boldsymbol{\eta}(\frac{dE}{ds})}}$$

- To minimize the time spread, the Dipole and Wedge Absorber operate isochronously to the end of the absorber.
- To mitigate large transverse spread of the beam out of the Rectilinear channel in the bending plane, edges of the dipole are contoured to focus muons with P_{max} and P_{min} of all input angles to be focused parallel upon dipole exit with muons of all momenta that enter the dipole on the reference path.
  - Transverse beam spread is reduced compared to free drift.
  - Enhanced co-linear beam allows for better focusing downstream.
- To mitigate large transverse spread in the non-bending plane, paired dipoles of opposite polarities create magnetic gradient fields that reduce the vertical spread of the beam.
- An iterative procedure to determine the absorber shape and isochronous configuration (θ bend of reference in dipole) optimizes for overall 6D cooling.

Summary

- Potential reduction of σ_E is estimated to be approximately by a factor of 10, but will be dependent on amount of transverse cooling yet to be estimated.
  - $\sigma_{E|Eq}$(Rectilinear) = 39.9 MeV to $\sigma_{E|Eq}$ = ~3.1 MeV?
- Can the reduction in $\sigma_{E|Eq}$ be useful to analyze the Higgs mass width (line shape) in the s-channel? Probably not sensitive to contribution of an individual particle, but maybe to addition or absence of a group of particles? Ask an HEP theorist?
  - In the 1990's, the line-shape of Z from LEP gave $N_\nu = 2.991 \pm 0.016$, providing a good argument that the top quark was the last quark to be discovered (or observed).

Backup

Overview: Input Parameters and Geometry 2/2

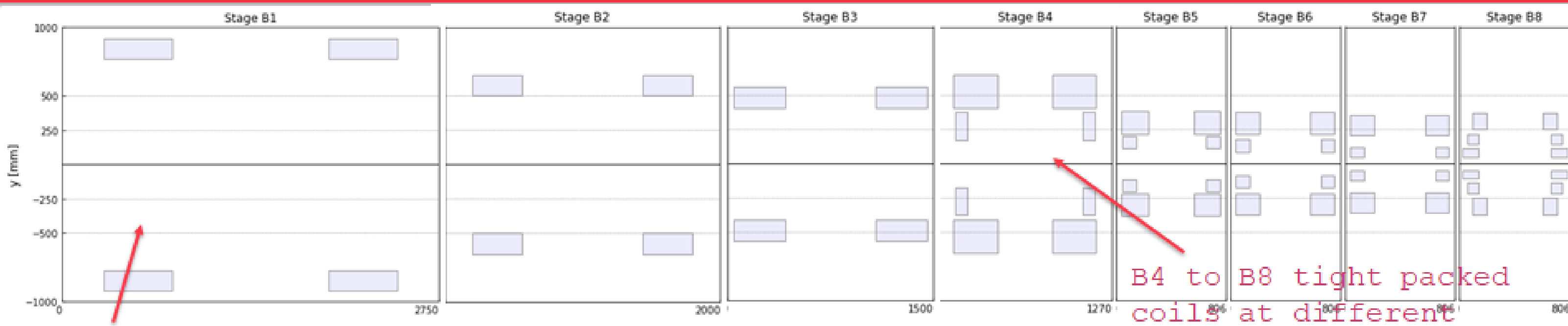

Large bore!

B4 to B8 tight packed coils at different radii!

Input Parameters		B1	B2	B3	B4		B5		B6		B7		B8		
		01	01	01	01	02	01	02	01	02	01	02	01	02	03
Bore Radius	mm	770	500	410	175	410	113	217	84	215	50	210	45	140	250
Magnet Thickness	mm	150	150	150	200	240	88	165	92	160	74	145	65	80	120
Magnet Length	mm	500	360	370	92	320	100	196	100	177	100	170	120	80	100
Current Density	A/mm^2	69.8	90	123	94	70.3	157	168	185	155.1	198	155	220	135	153
Cell Length	m	2.75	2	1.5	1.27		0.806		0.806		0.806		0.806		

15/05/2023 IMCC Accelerator Design Meeting

International MUON Collider Collaboration

Overview: Input Parameters and Geometry 1/2

CERN

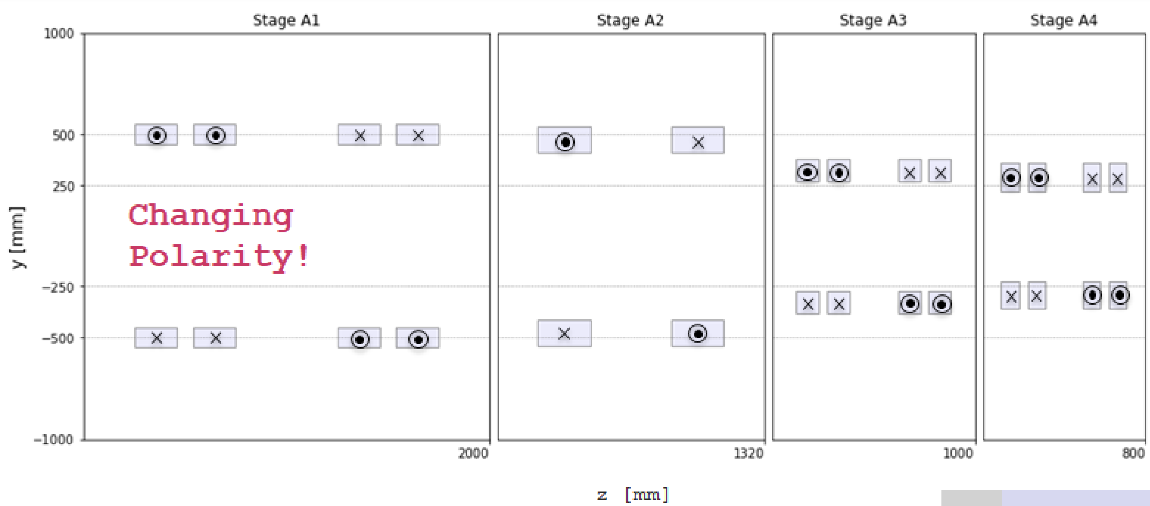

Input Parameters		A1 01	A2 01	A3 01	A4 01
Bore Radius	mm	450	410	270	220
Magnet Thickness	mm	100	130	110	140
Magnet Length	mm	210	260	110	90
Current Density	A/mm^2	63.25	126.6	165	195
Cell Length	m	2	1.32	1	0.8

15/05/2023 IMCC Accelerator Design Meeting 7

Snippets of Transverse Cooling Formulae from Dave Neuffer's CERN yellow book "CERN 99-12"

The differential equation for rms transverse cooling is [1]–[5]:

$$\frac{d\epsilon_N}{ds} = -\frac{1}{\beta^2 E}\frac{dE}{ds}\epsilon_N + \frac{\beta\gamma\beta_\perp}{2}\frac{d\langle\theta_{rms}^2\rangle}{ds} = -\frac{1}{\beta^2 E}\frac{dE}{ds}\epsilon_N + \frac{\beta_\perp E_s^2}{2\beta^3 m_\mu c^2 L_R E} \qquad (4.1)$$

where the first term is the energy-loss cooling effect and the second is the multiple scattering heating term. Here ϵ_N is the normalized emittance, E is the beam energy, $\beta = v/c$ and γ are the usual kinematic factors, dE/ds is the energy loss rate, θ_{rms} is the rms multiple scattering angle, L_R is the material radiation length, $\beta_\perp$ is the betatron function, and E_s is the characteristic scattering energy ($\sim$ 13.6 MeV) [6]. [The normalized emittance is related to the geometric emittance $\epsilon_\perp$ by $\epsilon_N = \epsilon_\perp/(\beta\gamma)$, and the beam size is given by $\sigma_x = (\epsilon_\perp\beta_\perp)^{1/2}$.]

4.3 Cooling considerations

Some general considerations on the conditions for cooling, and the required absorbers and beam transports, can be developed from Eqs. (4.1) to (4.9). From Eq. (4.1) [with g_x from (Eq. 4.7)] we find an equilibrium emittance from setting the derivative to zero:

$$\epsilon_{N,eq} = \frac{\beta_\perp E_s^2}{2 g_x \beta m_\mu c^2 L_R (dE/ds)} \ . \qquad (4.11)$$

This represents the minimal obtainable emittance for a given material and focusing parameter $\beta_\perp$. From this expression, obtaining small emittance implies having small $\beta_\perp$ (strong focusing), as well as large L_R dE/ds (small multiple scattering) at the absorber. Table 4.1 displays parameters of typical cooling materials; large L_R dE/ds implies light elements (H, Li, Be, etc.) for the absorber material.

Beneficial Aspects of Design Concepts

- Isochronous Dipole/Wedge Monochromator minimizes σ_t, which helps minimize the longitudinal emittance. Any increase in time spread of the beam occurs between the wedge exit and entry to RF, which is helpful for stable RF operation; and its growth is limited by the RF.
  - From the CERN 99-12 yellow paper on "μ^+–μ^- Colliders" by Dave Neuffer:

The minimum longitudinal emittance depends on the product of bunch length and energy spread. Longitudinal focusing can be varied substantially, depending on the RF wavelength and gradient, as well as the transport isochronicity. However, from recent studies, cooling to bunch lengths of ~ 1 cm seems readily achievable. A 3% energy spread at $E_\mu \cong 250$ MeV ($\sigma_E \cong 7.5$ MeV) obtains a normalized longitudinal emittance of:

$$\epsilon_{L,N} = \frac{\sigma_{ct}\sigma_E}{m_\mu c^2} \cong 0.0007 \text{ m} . \quad (4.14)$$

???

- Comparison to solenoid based cooling:
  - Avoids "canonical angular momenta build-up" that are due to the dispersed centers of Larmor orbits.
  - In this large dispersion scheme, is the impact of space charge reduced due to larger transverse separation over much of the channel? Answer will depend on future 4D cooling studies in region at de-focusing quad to RF where beam is transversely small.
  - A solenoid based cooling channel is needed for initial 6D cooling, since the baselined front-end capture system is solenoid based with benefit of capturing both signs.
  - However, if a non-baseline horn-based capture system is considered, this 6D cooling system might also be contemplated after initial 4D transverse cooling.

Addressing Vertical Spread

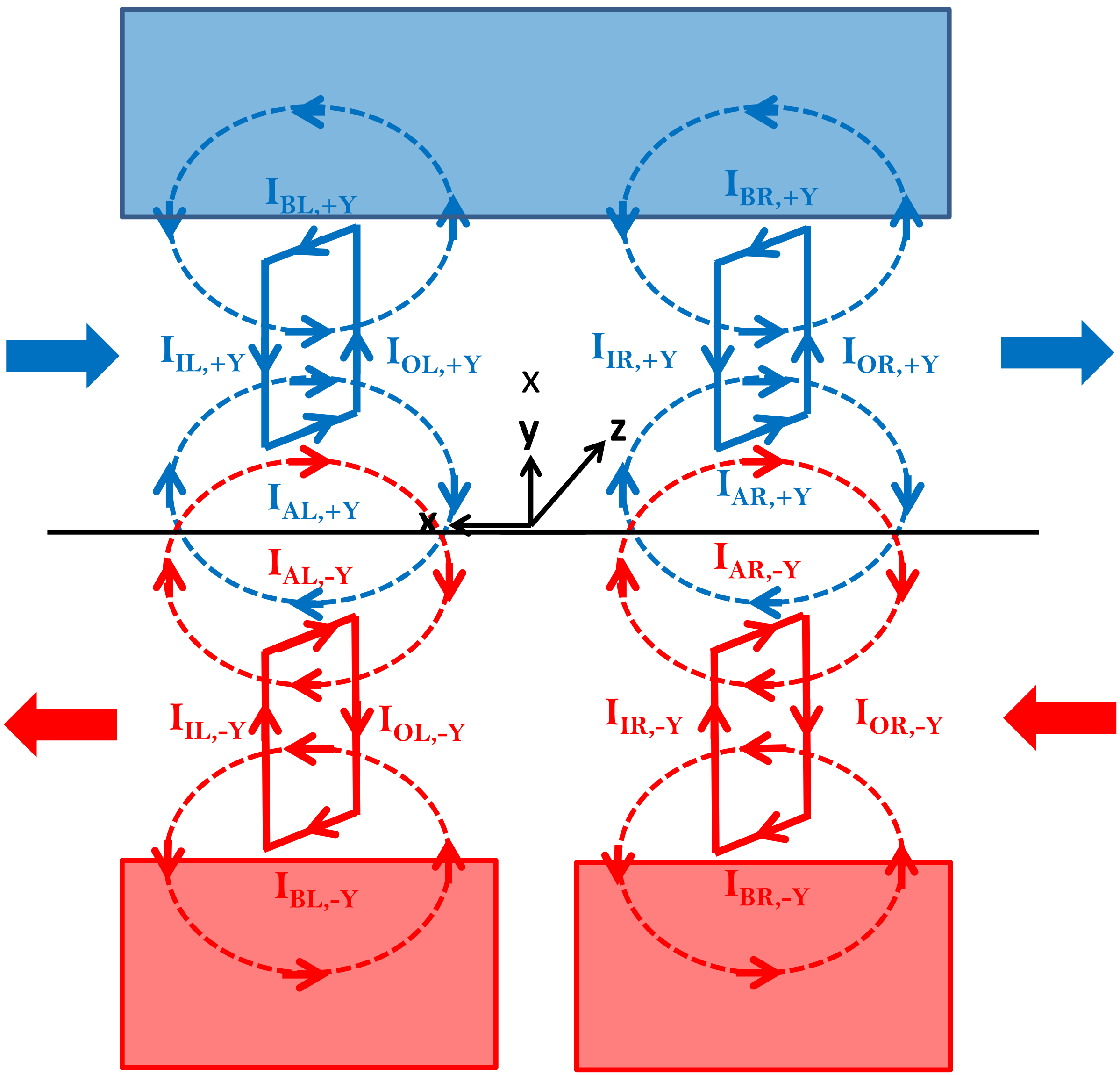

$$m = \frac{\sin\theta}{1-\cos\theta}$$

$$x_0 = \frac{2R(\cos\varphi + m\sin\varphi)}{1+m^2}$$

$$y_0 = m x_0$$

$$\frac{dy}{dx} = m_i = \frac{-1(x - R\cos\varphi)}{\sqrt{R^2 - (x - R\cos\varphi)^2}}$$

i = 0; RL,Hi; RL,Lo

$$x_{0,RL,HiP} = \pm\frac{m_0 R_{Hi}}{\sqrt{1+m_0^2}} + R_{Hi}\cos\varphi$$

$$y_{0,RL,HiP} = \pm\sqrt{R_{Hi}^2 - (x_{0,RL,HiP} - R_{Hi}\cos\varphi)^2} + R_{Hi}\sin\varphi$$

$$x_{1,RL,HiP} = \frac{y_{1,Hi} - y_{0,RL,HiP} + m_0 x_{0,RL,HiP} + \frac{x_{1,Hi}}{m_0}}{m_0 + \frac{1}{m_0}}$$

$$y_{1,RL,HiP} = y_{1,Hi} + \frac{-1}{m_0}(x_{1,RL,HiP} - x_{1,Hi})$$

$$m_{RL,Hi} = \frac{y - y_{0,FS,Hi}}{x - x_{0,FS,Hi}} = -0.1125$$

W_{total} = 8.75 cm

$$m_0 = \frac{y_{1,Hi} - y_{0,Hi}}{x_{1,Hi} - x_{0,Hi}} = \frac{y_{1,Lo} - y_{0,Lo}}{x_{1,Lo} - x_{0,Lo}} = 0.0856$$

$W_{total,P}$ = 8.47 cm

RL: RectiLinear

$\phi_{max} = \tan^{-1}(40/200)$
$= 11.3^o$

$$x_{1,RL,Hi} = \frac{y_{1,Hi} - y_{0,RL,Hi} + m_{RL,Hi} x_{0,RL,Hi} + \frac{x_{1,Hi}}{m_0}}{m_{RL,Hi} + \frac{1}{m_0}}$$

$$y_{1,RL,Hi} = y_{1,Hi} + \frac{-1}{m_0}(x_{1,RL,Hi} - x_{1,Hi})$$

$$m_{0,RL,HiP} = \frac{y_{0,RL,HiP} - y_{0,Hi}}{x_{0,RL,HiP} - x_{0,Hi}}$$

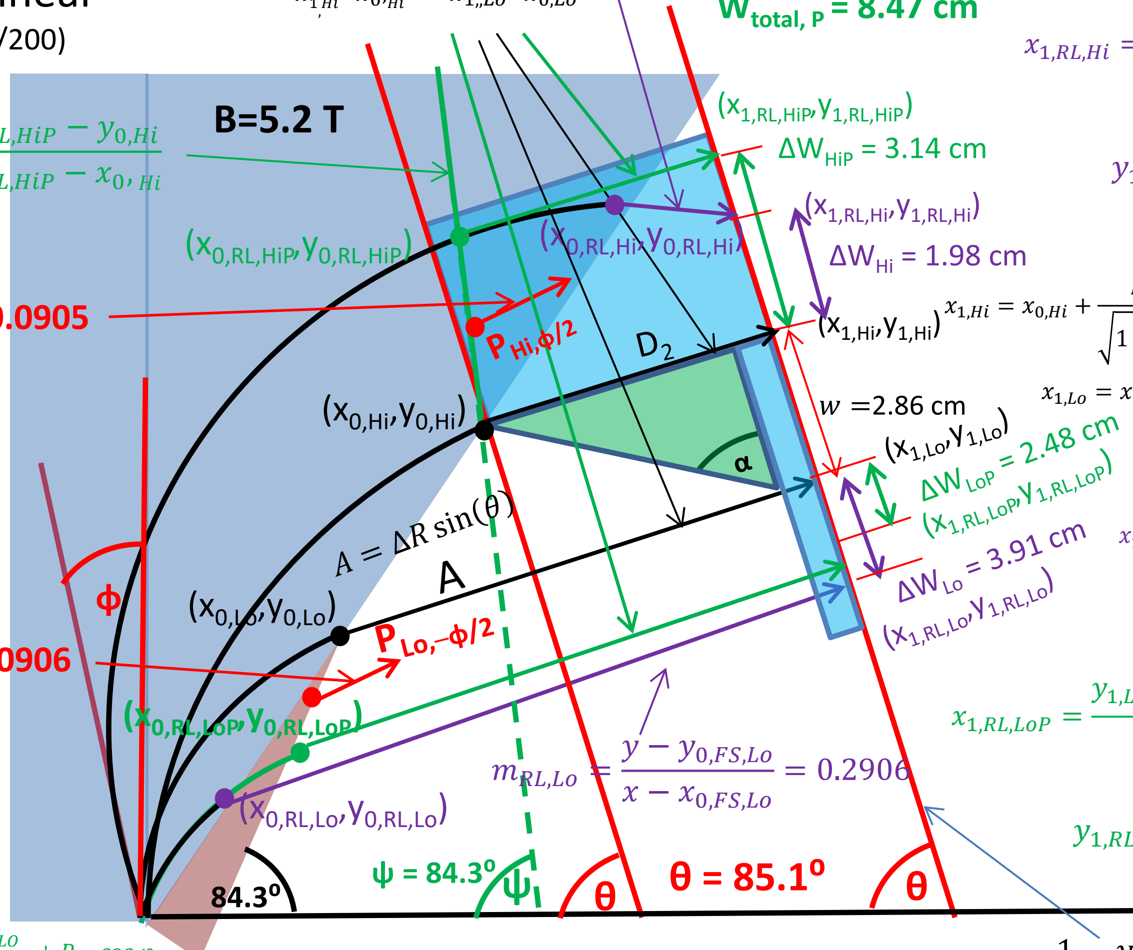

$$x_{1,Hi} = x_{0,Hi} + \frac{D_2}{\sqrt{1+m_0^2}} \qquad y_{1,Hi} = y_{0,Hi} + m_0(x_1 - x_{0,Hi})$$

$$x_{1,Lo} = x_{0,Lo} + \frac{A + D_2}{\sqrt{1+m_0^2}} \qquad y_{1,Lo} = y_{0,Lo} + m_0(x_{1,Lo} - x_{0,Lo})$$

$$x_{1,RL,Lo} = \frac{y_{1,Lo} - y_{0,RL,Lo} + m_{RL,Lo} x_{0,RL,Lo} + \frac{x_{1,Lo}}{m_0}}{m_{RL,Lo} + \frac{1}{m_0}}$$

$$y_{1,RL,Lo} = y_{1,Lo} + \frac{-1}{m_0}(x_{1,RL,Lo} - x_{1,Lo})$$

$$x_{1,RL,LoP} = \frac{y_{1,Lo} - y_{0,RL,LoP} + m_0 x_{0,RL,LoP} + \frac{x_{1,Lo}}{m_0}}{m_0 + \frac{1}{m_0}}$$

$$y_{1,RL,LoP} = y_{1,Lo} + \frac{-1}{m_0}(x_{1,RL,LoP} - x_{1,Lo})$$

$$m_{RL,Lo} = \frac{y - y_{0,FS,Lo}}{x - x_{0,FS,Lo}} = 0.2906$$

$$\frac{-1}{m_0} = \frac{y - y_{1,Hi}}{x - x_{1,Hi}} \qquad y = y_{1,Hi} + \frac{-1}{m_0}(x - x_{1,Hi})$$

$$x_{0,RL,LoP} = \pm\frac{m_0 R_{Lo}}{\sqrt{1+m_0^2}} + R_{Lo}\cos\varphi$$

$$y_{0,RL,LoP} = \pm\sqrt{R_{Lo}^2 - (x_{0,RL,LoP} - R_{Lo}\cos\varphi)^2} + R_{Lo}\sin\varphi$$

$$m = \frac{\sin\theta}{1-\cos\theta}$$

$$x_0 = \frac{2R(\cos\varphi + m\sin\varphi)}{1+m^2}$$

$$y_0 = m x_0$$

$$\frac{dy}{dx} = m_i = \frac{-1(x - R\cos\varphi)}{\sqrt{R^2 - (x - R\cos\varphi)^2}}$$

i = 0; RL,Hi; RL,Lo

$$x_{0,RL,HiP} = \pm\frac{m_0 R_{Hi}}{\sqrt{1+m_0^2}} + R_{Hi}\cos\varphi$$

$$y_{0,RL,HiP} = \pm\sqrt{R_{Hi}^2 - \left(x_{0,RL,HiP} - R_{Hi}\cos\varphi\right)^2} + R_{Hi}\sin\varphi$$

$$x_{1,RL,HiP} = \frac{y_{1,Hi} - y_{0,RL,HiP} + m_0 x_{0,RL,HiP} + \frac{x_{1,Hi}}{m_0}}{m_0 + \frac{1}{m_0}}$$

$$y_{1,RL,HiP} = y_{1,Hi} + \frac{-1}{m_0}\left(x_{1,RL,HiP} - x_{1,Hi}\right)$$

$$m_{RL,Hi} = \frac{y - y_{0,FS,Hi}}{x - x_{0,FS,Hi}} = -0.1125$$

$$m_0 = \frac{y_{1,Hi} - y_{0,Hi}}{x_{1,Hi} - x_{0,Hi}} = \frac{y_{1,Lo} - y_{0,Lo}}{x_{1,Lo} - x_{0,Lo}} = 0.0856$$

W_{total} = 8.75 cm

$W_{total,P}$ = 8.47 cm

RL: RectiLinear Backup

$$x_{1,RL,Hi} = \frac{y_{1,Hi} - y_{0,RL,Hi} + m_{RL,Hi} x_{0,RL,Hi} + \frac{x_{1,Hi}}{m_0}}{m_{RL,Hi} + \frac{1}{m_0}}$$

$$y_{1,RL,Hi} = y_{1,Hi} + \frac{-1}{m_0}\left(x_{1,RL,Hi} - x_{1,Hi}\right)$$

$$m_{0,FS,HiP} = \frac{y_{0,FS,HiP} - y_{0,Hi}}{x_{0,FS,HiP} - x_{0,Hi}}$$

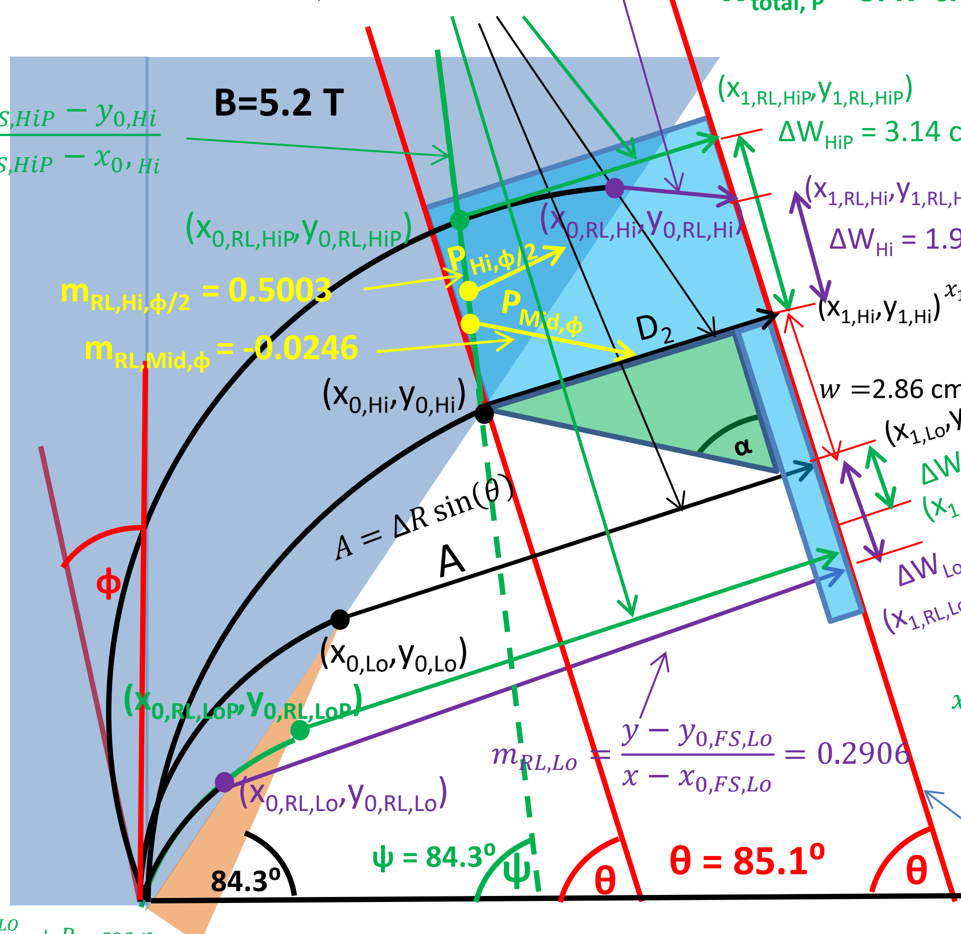

$$x_{1,Hi} = x_{0,Hi} + \frac{D_2}{\sqrt{1+m_0^2}} \qquad y_{1,Hi} = y_{0,Hi} + m_0(x_1 - x_{0,Hi})$$

$$x_{1,Lo} = x_{0,Lo} + \frac{A + D_2}{\sqrt{1+m_0^2}} \qquad y_{1,Lo} = y_{0,Lo} + m_0(x_{1,Lo} - x_{0,Lo})$$

$$x_{1,RL,Lo} = \frac{y_{1,Lo} - y_{0,RL,Lo} + m_{RL,Lo} x_{0,RL,Lo} + \frac{x_{1,Lo}}{m_0}}{m_{RL,Lo} + \frac{1}{m_0}}$$

$$y_{1,RL,Lo} = y_{1,Lo} + \frac{-1}{m_0}\left(x_{1,RL,Lo} - x_{1,Lo}\right)$$

$$x_{1,RL,LoP} = \frac{y_{1,Lo} - y_{0,RL,LoP} + m_0 x_{0,RL,LoP} + \frac{x_{1,Lo}}{m_0}}{m_0 + \frac{1}{m_0}}$$

$$m_{RL,Lo} = \frac{y - y_{0,FS,Lo}}{x - x_{0,FS,Lo}} = 0.2906$$

$$y_{1,RL,LoP} = y_{1,Lo} + \frac{-1}{m_0}\left(x_{1,RL,LoP} - x_{1,Lo}\right)$$

$$x_{0,RL,LoP} = \pm\frac{m_0 R_{LO}}{\sqrt{1+m_0^2}} + R_{Lo}\cos\varphi$$

$$y_{0,RL,LoP} = \pm\sqrt{R_{Lo}^2 - \left(x_{0,RL,LoP} - R_{Lo}\cos\varphi\right)^2} + R_{Lo}\sin\varphi$$

$$\frac{-1}{m_0} = \frac{y - y_{1,Hi}}{x - x_{1,Hi}} \qquad y = y_{1,Hi} + \frac{-1}{m_0}(x - x_{1,Hi})$$